Transportation Research Part D 100 (2021) 103045

Contents lists available at ScienceDirect

Transportation Research Part D

journal homepage: www.elsevier.com/locate/trd

Vulnerability patterns of road network to extreme floods based on accessibility measures

Tsolmongerel Papilloud [a,b,*], Margreth Keiler [c,d]

[a] University of Bern, Institute of Geography, Hallerstrasse 12, CH-3012 Bern, Switzerland
[b] University of Bern, Oeschger Centre for Climate Change Research, Mobiliar Lab for Natural Risks, Hochschulstrasse 4, CH-3012 Bern, Switzerland
[c] University of Innsbruck, Department of Geography, Innrain 52f, 6020 Innsbruck, Austria
[d] Austrian Academy of Sciences, Institute of Interdisciplinary Mountain Research, Innrain 25, 6020 Innsbruck, Austria

ARTICLE INFO

Keyword:
Accessibility-based vulnerability
Extreme flood impacts
Influence of applied parameters
Average shortest travel time path
Network analysis

ABSTRACT

Accessibility is a key measure of the vulnerability of road networks to disruptions such as floods. However, studies comparing the contribution of parameters to the accuracy of accessibility-based vulnerability assessment are lacking. We propose modifying two accessibility measures to include flood-affected populations, opportunities, and average shortest travel time. We also applied three methods including the divergent ranking method to identify the direct impact of extreme floods on road networks. The shortest travel time pathway calculation was enhanced with the inclusion of spatially distributed settlements as an input. The results indicate a strong relationship between parameter weights and the accessibility measures, irrespective of the evaluated approaches. The results of the study highlight that measures of overall vulnerability, with respect to inter-comparisons of flood scenarios alone, do not fully capture the local vulnerability of some traffic zones. This is particularly evident with the flooding of highly connected roads that serve these zones.

1. Introduction

Assessing vulnerability of transportation infrastructure to extreme floods is a growing field with continued advancements in flood modelling and network analysis techniques. Given the availability of high-resolution data on extreme floods, road networks and populations, the objective of this study is to improve the accuracy of accessibility-based vulnerability analysis of road networks at the regional scale. We propose to modify the existing vulnerability approaches and compare their results to the original approaches. Our specific contributions include investigating different measures to capture direct flood impacts to road networks and incorporating more information about the local road network in the accessibility-based vulnerability analysis. This is accomplished by modifying the way travel time between traffic zones is calculated. Moreover, we consider additional contributing factors to the accessibility-based vulnerability analysis by including number of residents and opportunities in flood-affected areas and investigate their effects in two different approaches.

* Corresponding author at: University of Bern, Institute of Geography, Hallerstrasse 12, CH-3012 Bern, Switzerland.
E-mail addresses: tsolmongerel.papilloud@giub.unibe.ch (T. Papilloud), margreth.keiler@uibk.ac.at (M. Keiler).

https://doi.org/10.1016/j.trd.2021.103045

Available online 6 October 2021

1.1. Background

Compared to the impact of different natural hazards, floods result in a significantly high percentage of damages. In recent years (1998–2017), more than US$ 656 billion of global economic losses were related to flood occurrences (CRED and UNISDR, 2018). Flood damages are expected to continue to increase in the future with respect to the state of socio-economic developments and climate change (Alfieri et al., 2017; Fuchs et al., 2015; Fuchs et al., 2017; Hoegh-Guldberg et al., 2018). Studies based in Europe showed that impacts to infrastructure are expected to make up a high ratio of the overall losses (Bubeck et al., 2011, Thieken et al., 2016). Furthermore, the disruption and reduced accessibility to critical infrastructure, such as transport networks, impacts the overall functionality of affected communities (Zischg et al., 2005a), such as population mobility (Zischg et al., 2005b) and, thus, economic development (Hallegatte et al., 2019; Schlögl et al., 2019). Understanding the different dimensions of vulnerability to floods is instrumental to gaining knowledge about flood impacts, to guide the development of appropriate risk analysis methods and to make critical decisions in risk management (Birkmann et al., 2013). Considering vulnerability assessments to infrastructure to date, this field is still in its infancy compared with other economic sectors and development is often limited by data availability (Bubeck et al., 2019).

Vulnerability assessment of complex systems, such as transportation infrastructure, requires the use of an integrated framework, which should include various analytical methods to investigate the problem from a range of perspectives. These consider topological, functional, logical and dynamic properties (Cantillo et al., 2019; Unterrader et al., 2018; Zio, 2016). Significant work is still needed to identify differences in vulnerability across space, time and systems (Grubesic & Matisziw, 2013). According to the UNISDR (2016:24), vulnerability is defined as "the conditions determined by physical, social, economic and environmental factors or processes, which increase the susceptibility of an individual, a community, assets or systems to the impacts of hazards". Thus, in general, a vulnerability analysis includes consequences of a certain flood event and can be expressed in terms of functions, indicators and indices (Fuchs et al., 2019), depend on data availability (Malgwi et al., 2020) and the decision-making context (Papathoma-Köhle et al., 2019). Vulnerability has also taken on a different meaning in road infrastructure studies: Jenelius et al. (2006) argue that the concept of vulnerability with respect to road infrastructure should address two components: probability of hazard occurrence and consequences of the hazard event. Furthermore, Jenelius and Mattsson (2015) state that the impact for a single user under a certain disruption scenario is considered as a function of the exposure of a user to that scenario. The same description of the context is named as vulnerability by Taylor and Susiliwati (2012). However, Berdica (2002:119) defines vulnerability more specifically to "the susceptibility to incidents that can result in considerable reductions in road network serviceability". Moreover, Taylor (2008) defines network vulnerability based on road accessibility to activities from different locations within a regional network. In this context, accessibility is defined as the ease with which services and facilities can be reached while using the road network (Litman, 2008). A broad overview on studies considering transport resilience and vulnerability, and the role of connectivity and accessibility is provided by Reggiani et al. (2015).

Floods can cause disruptions to roads that leave transportation networks partially operational to completely blocked, which can result in notable service delays (Pregnolato et al., 2017). Chen et al. (2015) highlight certain gaps in current research on flood vulnerability assessment of transport networks. For example, reductions in road capacity due to hazard events are not yet considered. To address this issue, Pregnolato et al. (2017) recommended applying the flood-depth disruption function, which identified certain water depths as thresholds that correlate to the loss of vehicle control when water levels rise to the bottom of most personal vehicles. These thresholds are defined at different levels such as 15 cm (Pearson and Hamilton, 2014), 20 cm (Pyatkova et al., 2015), 30 cm (Yin et al., 2016), and up to 90 cm for four wheel drive vehicles (Pregnolato et al., 2017).

These newly developed approaches also acknowledge the importance of considering geographic scales, the topological structure of infrastructure and flood exposure (e.g., Papilloud et al. (2020)) when assessing infrastructure vulnerability (Grubesic & Matisziw, 2013). Consequences to road users differ in flood exposed areas as a result of these contributing characteristics. For example, increased travel times and distances, and changes in traffic flow play major roles in the vulnerability assessment of transport infrastructure (Jenelius et al., 2006, Taylor et al., 2006). One of the topological measures, which indicates connectivity in the network, is edge betweenness centrality (Girvan and Newman, 2002). If an edge is connecting clusters in the network, then it has high edge betweenness centrality. Kermanshah and Derrible (2017) used the difference of mean edge betweenness centrality of a road network calculated for pre- and post-flood events to quantify the impact of extreme floods on connectivity. Furthermore, Casali and Heinimann (2019b) applied edge betweenness centrality of road network in city of Zurich to evaluate the impacts of two different flood scenarios on changes in the network after the flood occurrences.

Hasan and Foliente (2015) highlight a potential research challenge to assess the vulnerability of infrastructure to disruptions, to better understand more extensive impacts on the people and communities in and around the occurrences. One way to understand the impacts of transportation infrastructure disruptions on people could be the accessibility-based vulnerability approach. This examines changes of access levels across a disrupted network (Taylor, 2017), thereby providing insight on the impacts to a broader range of socio-economic aspects and to the society as a whole. Moreover, Caschili et al. (2015) recommend conducting comparisons of different vulnerability indices at variable spatial scales. Given the identified gaps and challenges, the following section provides a more detailed overview of recent studies within the scope of accessibility-based vulnerability assessment.

1.2. Previous studies on accessibility-based vulnerability assessment

In general, accessibility-based studies increased rapidly in the period between 2000 and 2019 and mainly address the categories of newly developed indicators and accessibility-based applications for social equity, transportation network planning, and travel behaviour (Shi et al., 2020). Considering vulnerability, different types of accessibility measures for road networks can be characterized by combining different dimensions of the transport system (impedance, e.g., travel time or distance) and certain land use patterns

Table 1
Attractiveness and type of Hansen accessibility measure.

Reference	Specific feature of accessibility index	Attractiveness weight parameter 1 (for zone *i*)	Parameter 2 (other zones *j*)	Deterrent function (or function of distance decay)
Taylor et al. (2006)	Normalized Hansen Index	1 (no weight)	Sum of population in all cities (except *i*)	Inverse of travel distance
Chen et al. (2015)	Normalized Hansen Index modified with travel modes (two different travel modes: cars and high-occupancy vehicles)	Employment places and schools	Sum of population in all zones (except *i*)	Exponential function of travel distance
Borowska-Stefańska et al. (2019)	Normalized Hansen Index with mobility considerations (i.e. changes to travel time), with focus on traffic speed and flow changes	Employment places (not explicitly specified in the literature)		Exponential function $f_{dd} = \exp(-\beta t_{ij})$ f_{dd} – distance decay t_{ij} – travel time between regions β – beta parameter
Noland et al. (2019)	Hansen index without normalization	Population	Sum of available jobs in all census block-groups (census blocks are aggregated to census block-group)	Inverse of travel distance

(accessibility, e.g., attractiveness, opportunity or activity). The five main types of measures are categorized as dimensions of spatial separation, cumulative opportunity, gravity-based, utility-based, and time–space (Miller, 2018; Silva et al., 2019). Spatial separation only accounts for the distance. Cumulative opportunities measure those within a defined travel time. Utility measures consider different travel choices and individual perceptions the time–space measure focuses on individual time constraints. Among these types, the gravity-based measure considers the attractiveness of a zone and an impedance parameter between zones, where the latter can represent either the distance or travel time. A range of factors may influence the attractiveness of a given location for an activity. A simplified way to measure attractiveness could be by the number of people living in a specific zone, under the working assumption that higher population density represents higher attractiveness. A zone can refer to an administrative area, such as a city or a county, or to an area demarcation that reflects a specific purpose such as a traffic zone or a census block. Consequently, it is a challenge to measure the attractiveness of a location given the heterogeneity of human activities (Miller, 2018).

Regarding the focus on the vulnerability of the road network due to floods, gravity-based measures are of particular interest due to the summation of opportunities in a given zone and the addition of a penalty term that accounts for increasing time or distance from the zone.

The gravity-based accessibility measure includes the Hansen accessibility index. It was first proposed by Hansen (1959) and has been widely applied to urban planning and social science studies to measure the accessibility to certain locations such as emergency services and employment ones (Gori et al., 2020; Noland et al., 2019). Since we are going to analyse accessibility-based vulnerability of road networks to floods based on spatial distribution of population and opportunities, we choose the following two variations of the Hansen indices. The first one is referred to as the normalized Hansen integral accessibility index (Taylor, 2017). It is defined as:

$$A_i = \frac{\sum_j B_j f(C_{ij})}{\sum_j B_j}, \tag{1}$$

where,

A_i is the normalized Hansen integral accessibility index, normalized by total attractiveness, for zone i;
B_j is the attractiveness of zone j; (e.g., the number of opportunities available at j); and
$f(C_{ij})$ is the impedance function that represents the separation between the two zones.

The results of applying the normalized Hansen measure are dependent on parameters chosen for B_j and the impedance function. For example, this normalized version was used by Taylor et al. (2006), and the attractiveness was represented by the population of city j.

The impedance function can be defined as an inverse relationship with respect to travel cost or as an exponential function depending on travel cost, so that the higher the cost of travel between two zones, the lower the accessibility between them. Taylor et al. (2006) defined the impedance function as

$$f(C_{ij}) = \frac{1}{x_{ij}}, \tag{2}$$

where x_{ij} is the travel distance between two cities.

Parameters for describing the opportunity or attractiveness with the normalized Hansen index vary in different studies. An overview of feasible values and applications of these parameters are summarized in Table 1. Almost all of these studies applied the normalized Hansen index during flood-attributed disruptions, except for Taylor et al. (2006), which consider generic disruptions. To compare Hansen accessibility indices between the flood event and pre-flood conditions, Taylor et al. (2006) used relative values of the

Hansen index (percentage of change), which are ratios between the index of the degraded network due to floods and the index of pre-flood network. Noland et al. (2019) use percent reduction to compare accessibility indices that correspond to both the flood event and to pre-flood conditions.

The studies also differ with respect to the applied impedance function. Accessibility analysis by Noland et al. (2019), for instance, used the shortest distance, while Borowska-Stefańska et al. (2019) used the travel time between regions.

In the studies summarized in Table 1, the number of employment places in a defined zone was mostly used as an indicator of attractiveness. Other commonly adapted attractiveness parameters have included total population, numbers of households and/or vehicles, the number of employment places, hospital beds, surgeons, and schools within a defined zone (Basso et al., 2020; Geurs & van Wee, 2004). These parameters can be further categorized as indicators of:

- daily attractiveness (based on e.g. the employment density, the number of schools, students, etc.);
- leisure attractiveness (based on e.g. the number of visitors to parks and museums, etc.); and
- critical service availability (e.g. the number of hospital beds within a zone).

The second Hansen measure is referred to as the population weighted Hansen index (Wachs and Kumagai, 1973), where the population residing in the defined study area is factored in as follows:

$$A_i^P = P_i \sum_j B_j f(C_{ij}) \tag{3}$$

In Eq. (3), the population of the zone of interest i (P_i), is included as a weight to calculate the accessibility therein.

Evaluating studies based on Hansen accessibility measure to assess the changes of transport networks during flood events (accessibility-based vulnerability) are known to have two main limitations: (i) the applied methods exclude the influence of population and opportunities under flood-affected areas, and (ii) these studies considered changes along the shortest distance and/or the shortest travel time paths between two zones or between a critical facility and a zone. Disregarding the contributing factors in flood-affected areas impacts the ability to properly define the scale and focus when conducting vulnerability analyses. For example, studies by Taylor and D'Este (2007) and Sohn (2006) conducted at national and state levels, respectively, both focus on accessibility between cities (Sohn, 2006; Taylor & D'Este, 2007). In these studies, it was acceptable to assess accessibility between cities because of the large scale; although it oversimplifies the reality because there could be directly and indirectly affected people in both direct and indirect due to flood-induced disruptions in the areas, especially where there are high population densities.

Chen et al. (2015) improved the normalized Hansen integral index by incorporating different modes of transportation, such as by cars and by high-occupancy vehicles to address effect of population weight. However, findings from this study also showed that integration of flood-affected populations and opportunities into the accessibility-based vulnerability is lacking.

Further developments for evaluating flood impact on accessibility are shown by Gori et al. (2020). They applied (i) the shortest distances between critical facilities (i.e., hospitals and fire stations) and census block-groups, and (ii) they introduced Connectivity loss $CL_{O\to D}$, which corresponds to a measure of efficiency reduction when traversing along an origin–destination (OD) pair on a disrupted road network. In particular, $CL_{O\to D}$ is mathematically expressed as

$$CL_{O\to D} = 1 - \frac{L_{O\to D}^{undisturbed}}{L_{O\to D}^{flood}}, \tag{4}$$

where $0 \leq CL_{O\to D} \leq 1$, and $L_{O\to D}^{undisturbed}$ and $L_{O\to D}^{flood}$ denote the lengths of the shortest OD path for the undisrupted and the flood induced road network, respectively.

Another accessibility-based measure is referred to as the accessibility score (Sohn, 2006), which incorporates the effects of the impedance function and traffic volume. However, these further developments of the assessment still also have limitations. Firstly, local roads are not considered as possible detours during flood events. Secondly, since cities are represented as points instead of areas, populations within these cities are aggregated to a single node for accessibility calculations. Hence, we argue that for flood vulnerability analysis, (i) population and opportunities affected by flood parameters should be considered specifically in the weight of the Traffic Zone (TZ) in different Hansen indices, and (ii) results will be meaningful at the regional scale when considering different travel routes. Another factor is that populations residing beyond flooded areas may be able to relocate with some additional travel time, while populations directly impacted by flooded areas may not be able to relocate at all. Therefore, accounting for flood-affected populations of a given TZ in the vulnerability calculation improves the accuracy of the Hansen index during flood condition.

Regarding the second limitation mentioned above, cities are typically represented as single point (node) locations at more synoptic geographic scales. Therefore, it is common to use the shortest distance or shortest travel time paths between single point representations of these cities. The single point is also used when describing accessibility from a zone to certain facilities. Moreover, calculating only the shortest distance path or the shortest travel time path between zones of interest disregards other possible routes between zones. For example, if a road user wishes to travel from the furthest location of one zone to another zone, the travel time would increase considerably. Considering these possibilities, utilizing average travel time or average shortest distance between zones would offer the possibility to further improve the accuracy of the vulnerability analysis.

Besides these two aforementioned limitations, Neumann et al. (2015) noted a need to consider extreme events in the vulnerability analysis. Increases in precipitation extremes (Hoegh-Guldberg et al., 2018) that could cause extreme floods and damage, call for more research on the accurate assessment of infrastructure vulnerability to floods. The direct impact of floods on the road network is highly

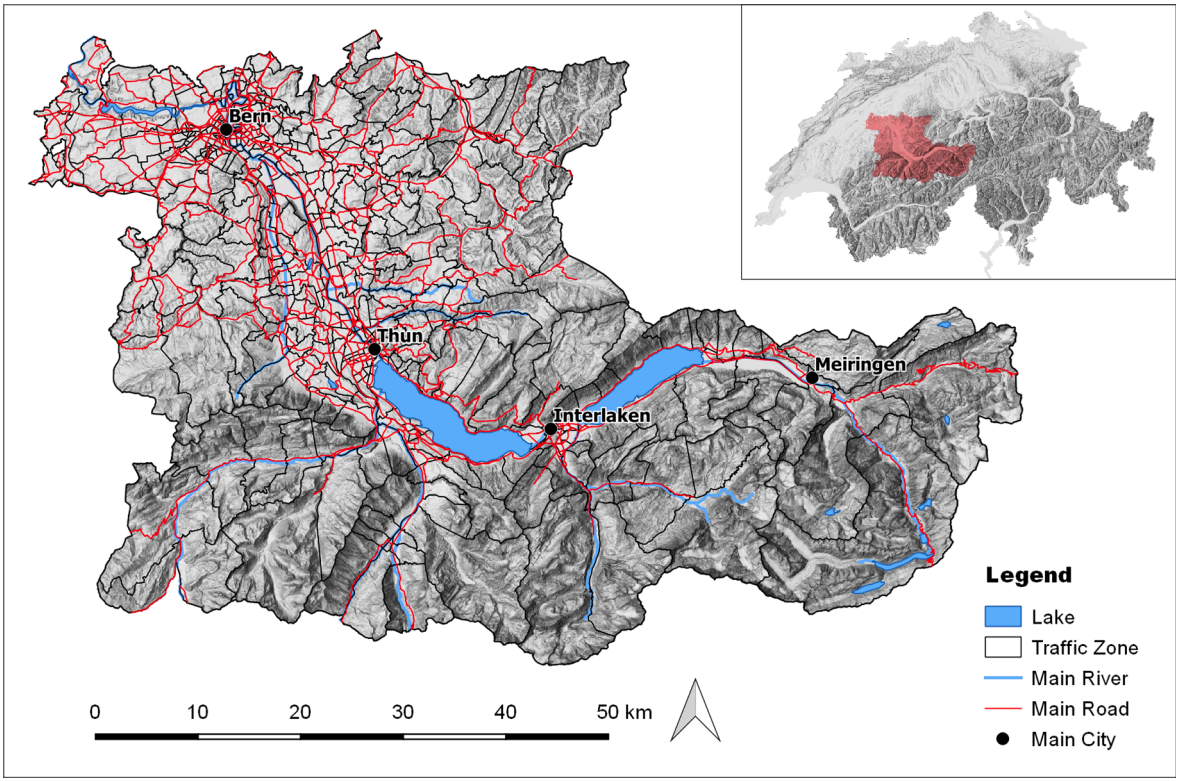

Fig. 1. Location of the study area within Switzerland and overview on major road network, traffic zones, main rivers and main cities (Major road network and traffic zones provided by (ARE, 2020), main rivers and main cities are from SwissTLM3D dataset provided by (Federal Office of Topography, 2019)).

dependent on how important road connections are affected. Thus, accessibility-based vulnerability can be affected by key road segments that are impacted during a given extreme flood event. Overall, Shi et al. (2020) stated that there is a need for future research to focus on comparative accessibility studies to select for more suitable approaches to be applied and for the inclusion of the impedance function with respect to the purpose of the study and the spatial context.

Taking all the identified gaps and opportunities into consideration, the overall objective of this study is to improve the accessibility-based vulnerability analysis of road networks at the regional scale.

The study is divided in two parts with the following specific aims:

Part 1. Direct impacts of extreme floods to the road network

- to investigate different measures of extreme flood impacts to the road network.

Part 2. Indirect impacts of extreme floods to the road network

- to incorporate more information about the local road network in the accessibility-based vulnerability analysis by modifying the approach to calculate travel time between zones;
- to include additional contributing factors to the accessibility-based vulnerability analysis by including the number of residents and opportunities in flood-affected areas;
- to effectively identify the most vulnerable traffic zones with respect to selected extreme flood scenarios; and
- to investigate the effects of the following factors on accessibility-based vulnerability assessment: different measure of population, opportunity, average travel time between zones, as well as the impact of flood scenarios as a function of the topological structure of a given road network.

2. Data and methods

2.1. Study area and data

The study area to investigate the accessibility-based vulnerability assessment is located in the southern part of the canton of Bern, Switzerland (Fig. 1). It covers an area about 3500 km^2, which mainly overlaps with the Aare river catchment upstream of the city of

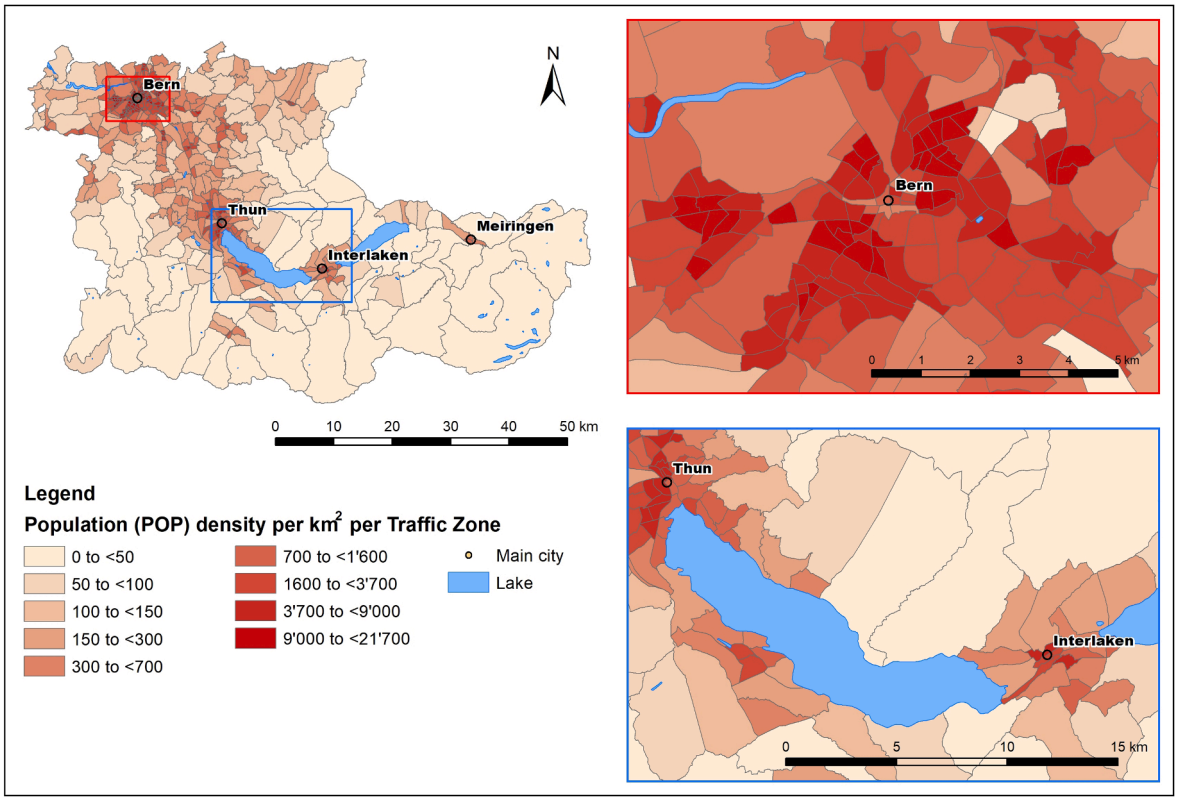

Fig. 2. Density map of population in traffic zones. Data provided by Federal Statistical Office (2016a).

Bern. The study area covers the high mountain areas of the Alps with elevations of up to 4200 m a.s.l. including glaciers (about 8% of the catchment are glaciated), to the hilly landscapes of the pre-Alps and the Swiss plateau. Flat and wide floodplains and two lakes (Lake Brienz, Lake Thun) prone to flooding characterize the Aare River. The fan of the river Lütschinen divides the two lakes, where the settlement of Interlaken is located. Further main rivers contributing to the Aare River are the Kander River (flowing into the Lake Thun) and the Gürbe River joining the Aare River between Thun and Bern (see Fig. 1).

The study by Zischg et al. (2018) assessed the impact of extreme floods on buildings in the Aare River basin. Probable maximum floods (PMF), based on a coupled model chain (hydrological, hydraulic, impact), were considered, starting with the probable maximum precipitation (PMP). To gain the different flood scenarios, the total precipitation based on the 3-day PMP was distributed in relation to spatial and temporal variations modelled with a Monte Carlo approach. Furthermore, the temporal pattern of the rainfall was distributed spatially in three meteorological regions, and in the sub-catchments of each meteorological region to mirror independent flood behaviour of specific parts of the catchment. An ensemble of 150 flood scenarios originally from the exhaustive number of Monte Carlo simulations were selected based on the highest discharge at the basin outlet in Bern. The latter is a main input in this study. Zischg et al. (2018) showed that the complex mountainous catchment has to be considered for analysing floods and induced damage. Moreover, they identified the highest lake level as the most severe contributing factor to flood damage to residential properties, rather than the maximum outflow discharge near Bern. However, the distribution of exposure also plays a crucial role on the severity of the consequences.

The road network (see Fig. 1) and the settlement areas are mainly concentrated in the valleys, thus in flood prone areas. The road network is more spread in the hilly landscapes. In the study area, 610,000 residents live distributed across 156 municipalities with lower population density but primarily in major cities such as Bern (141,500) and Thun (44,000) with higher population densities (see Fig. 2 population density). Fig. 3 presents the spatial distribution of opportunities such as employment and school places in the study area. The opportunity density map indicates regional differences as such larger cities like Bern and Thun, and there are more opportunities in their vicinities than in relatively more distant cities like Interlaken and Meiringen or even the more rural regions.

Different authorities provide the data in the study area in various formats; thus, pre-processing is needed. The road data is based on the TLM road data set represented as spatial polylines in an ArcGIS shape file, with detailed information on all road types, provided by the Swiss Topographical Office (Federal Office of Topography, 2019). Road weight is assigned as a width value to reflect the type of road (1 m until up to 12 m) in the TLM road dataset (Table A.1). We consider the feature to be a major road when its width is $\geq$6 m.

The Federal Office for Spatial Development (ARE) classify the road network in 531 high-resolution traffic zones in the area of interest (Fig. 1). Traffic zones were delineated with the aim to homogenize the distribution of inhabitants and employment places with a reduced variance from the mean value. These traffic zone are the basis for the Swiss Transport Model, which was generated from a

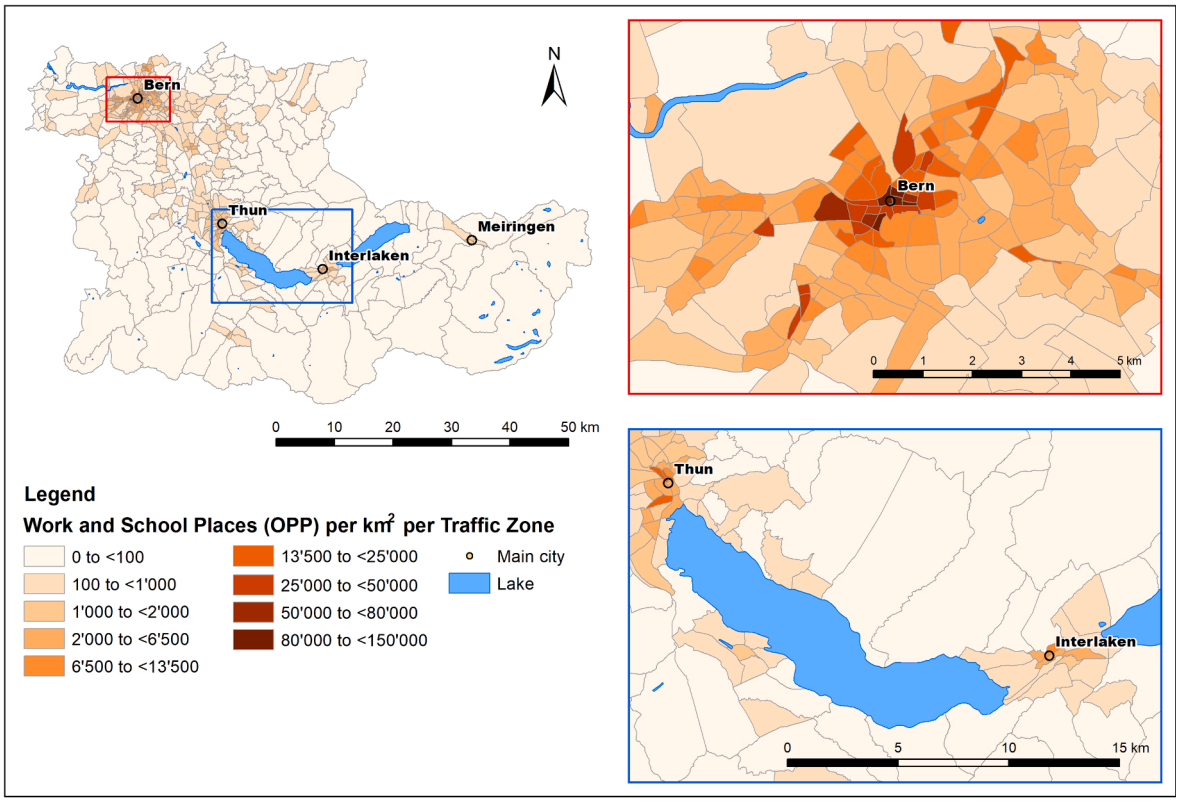

Fig. 3. Density map of opportunities in traffic zones. Data provided by Federal Statistical Office (2016b, 2017).

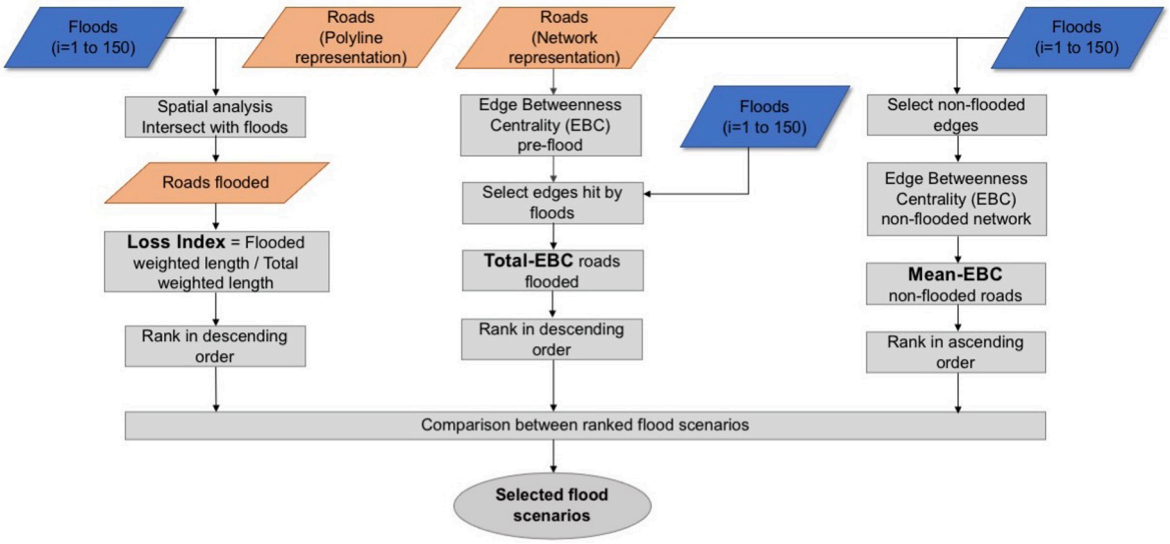

Fig. 4. Workflow with three different approaches for selecting flood scenarios for further investigations and comparison.

traffic analysis (ARE, 2020).

ArcGIS and Python scripts were used to perform spatial and data operations such as intersection, spatial and attribute joins. Network analysis was conducted with igraph python. For the spatial network analysis, the TLM road data set was converted from the ArcGIS shapefile into a directed weighted graph for further analysis in the igraph software. We assigned a weight to each edge as travel time according to the type of road in the TLM data set (Table A.1). This detailed road network supports the consideration of detour options of both major roads and the use of smaller municipal roads.

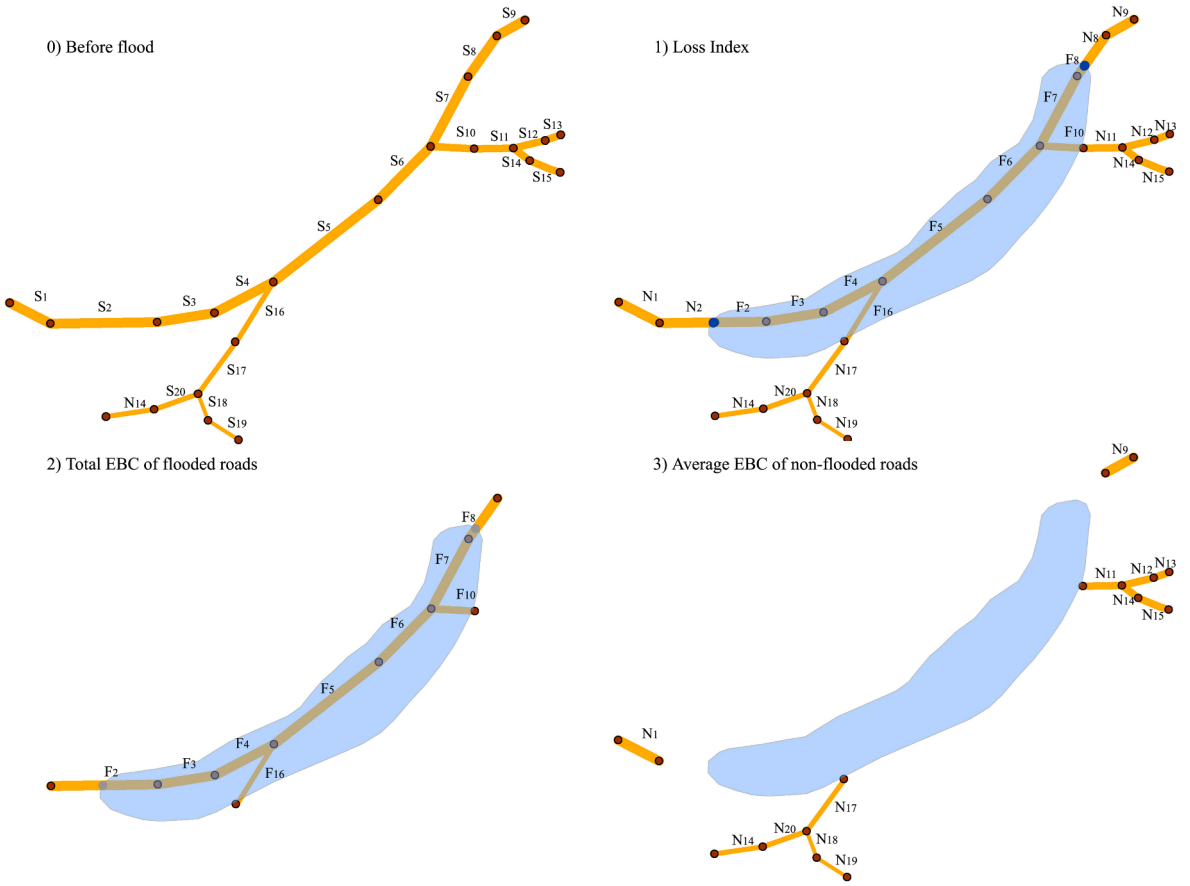

Fig. 5. Road segments in before and during flood conditions. (0) Before flood; (1) Flooded and non-flooded road segments: Fi-s are flooded road segments, and Ni-s are non-flooded road segments. A brown point represents a vertex (or a node in a graph) while a blue point represents a point that cut the original road segment by intersection of flood boundary. Blue point is illustrated in grey colour in the second method; (2) Road segments considered as flood-hit during floods for calculation of Total-EBC. Grey point is not a node in the graph; (3) Road segments considered as non-flooded during floods for calculation of Mean-EBC.

The 150 flood scenarios provided by Zischg et al. (2018) were intersected with the road network so that information on flood height at respective road segments could be included. If flood heights reach or exceed 20 cm, then the road segment is considered to be inaccessible to vehicles (Pregnolato et al., 2017). Consequently, the entire road section (modelled by end nodes and edge) is excluded from the network even if it is only partially covered by floods.

The Federal Statistical Office provided location-based data on local populations (Federal Statistical Office, 2016a), the number of work places (Federal Statistical Office, 2016b) and schools (Federal Statistical Office, 2017). Availability of detailed population data with respect to individual building footprints, employment and school places within traffic zones allows us to account for the number of people directly affected by floods (i.e., number of people located within a flood perimeter) in the accessibility calculation. The locations of working places and of schools are combined by summation to represent opportunities per traffic zone (see Fig. 2).

2.2. Measures for extreme flood impacts and their comparison

2.2.1. Measures for extreme flood impacts to the road network

We used three measures to assess flood impacts on the road network. Fig. 4 illustrates the methodological workflow for assessing flood impact scenarios.

The first is the **Loss Index** (LI) of flooded roads based on Gori et al. (2020), which identifies the percentage of weighted length of roads (i.e. road surfaces) that are directly impacted by floods. This indicates direct loss of access to parts of the traffic network. The LI index of flooded roads is calculated as follows:

$$LI = \frac{Flooded\ \ total\ \ weighted\ \ length}{Total\ \ weighted\ \ length}, \tag{5}$$

where the total weighted length equals the sum of all weighted road lengths. The weighted road length is defined as the multiplication

of road width and the road length (=road surface area). The road area is calculated for the whole road data set and for each flood scenario. In the example illustrated in Fig. 5(1) the LI is calculated as the ratio between total road area of flooded road segments F*i*-s and total road area of all road segments consisting of both N*i*-s and F*i*-s. Originally, N_2 and F_2 were parts of one road segment S_2. Intersection by the flood polygon divides segments into flooded and non-flooded parts. The different LI are ranked for the 150 scenarios in descending order, where the scenario with the maximum LI is ranked first.

The second approach is the total value of normalized edge betweenness centrality of flooded roads (**Total-EBC**), which indicates how many of important roads in terms of connectivity within the network are affected by floods (Girvan and Newman, 2002; Casali and Heinimann, 2019a). The normalized edge betweenness centrality measure (EBC) is defined (Girvan and Newman, 2002), as

$$EBC = \frac{1}{N(N-1)} \sum_{i \neq j} \frac{\sigma_{ij}(E)}{\sigma_{ij}}, \tag{6}$$

where σ_{ij} is the number of shortest paths from node i to node j, and $\sigma_{ij}(E)$ is the number of shortest paths from i to j that pass through edge E, and N is the total number of nodes.

Normalized EBC was calculated for the complete network prior to flood occurrence. For each flood scenario, the impacted road segments are extracted and the total normalized EBC values of these segments are added up. On the example of Fig. 5(2) the Total-EBC is calculated for the original graph including F_2 and F_8 (they are equal to S_2, S_8). 150 scenarios are then ranked by Total-EBC values in descending order, where the scenario with the maximum Total-EBC is ranked first. This represents the maximum loss of important roads to floods.

The third approach is the average normalized edge betweenness centrality values during flood occurrence (**Mean-EBC**), which is derived from the studies conducted by Kermanshah et al. (2017) and Kermanshah and Derrible (2017). In particular, this measure expresses how well remaining, functional roads perform, after the loss of other flood impacted road segments in the network. The normalized edge betweenness centrality is calculated under normal road network conditions (i.e., before flood occurrence) and during each of the 150 flood scenarios with degraded networks by removing the flood-affected road segments before re-calculation. On the example illustrated in Fig. 5(3) the average edge betweenness during flood condition is calculated for the remaining network after F_1, F_7 and other flooded roads were excluded from the original network. The flood scenario with the minimum Mean-EBC is then ranked first. The minimum Mean-EBC represents the maximum direct impact of floods on the remainder of the functional road network.

2.2.2. Selection criteria and comparison of extreme flood impacts

Among the 150 extreme flood scenarios, we chose different flood scenarios to analyse the vulnerability of road network further. Flood scenario selection is based on two different criteria. Firstly, we select flood scenarios with the highest rank for one of the three approaches, namely LI, Mean-EBC, and Total-EBC. Secondly, the correlation between the ranking of the three approaches is applied to define the basis for the subsequent selection criteria, which result in a notably different ranking (high differences) to analyse the influences (e.g., network topology, extend of flood) of the vulnerability assessment. It is defined as a difference between Mean-EBC and Total-EBC. The difference indicates how much the rankings of flood impacts to the rest of the network diverges from the total importance based on connectivity of flooded road elements.

Correlation tests are carried out between the results of the different measures using Spearman's rank order correlation (Weaver et al., 2017) in an R statistical analysis tool. Spearman's correlation test returns the strength of the relationship between two sets of variables. While the null hypothesis of Spearman's correlation test suggests that two variables are not associated, the alternative hypothesis suggests that there is a monotonic relationship that either indicates a positive or a negative relationship. Since LI is a ratio, we use Spearman's rank-order correlation test.

After selecting flood scenarios based on the ranking of three measures and divergent ranking between the measures, we compare the selected flood scenarios based on their geographic extents both quantitatively and qualitatively. Analyses consider flooded areas, flood affected road surfaces and traffic zones, and ratios between flood affected road surfaces and total road surfaces either by each flood scenario or by combination of flood scenarios. Combination of flood scenarios include a case that a road or a traffic zone affected by one specific scenario but not others based on logical combination of floods.

2.3. Accessibility indices and their comparison by flood scenario

The shortest travel times between zones are used as an impedance in the accessibility. After data pre-processing and the selection of flood scenarios, the calculation of the shortest travel times between zones was carried out before the accessibility-based vulnerability analysis could be conducted.

2.3.1. Identification of average shortest travel time paths between traffic zones

The impedance function in the Hansen index can represent either the shortest distance or the shortest travel time. Generally, both are calculated from one centroid starting point (node) of one zone to another centroid endpoint (node) in the other zone of interest within a network.

Our method differs in that each traffic zone is divided in a grid with 200 × 200 m raster cells with respect to the settlement pattern and selected a node of road network in each raster cell (see Fig. 6). Due to the increase of considered nodes in traffic zones compared to one centroid point, the shortest travel time paths were calculated using the network analysis tool igraph between each node of a given traffic zone to all nodes of another zone. These represent all possible travel times between the zones. In the next step, the average

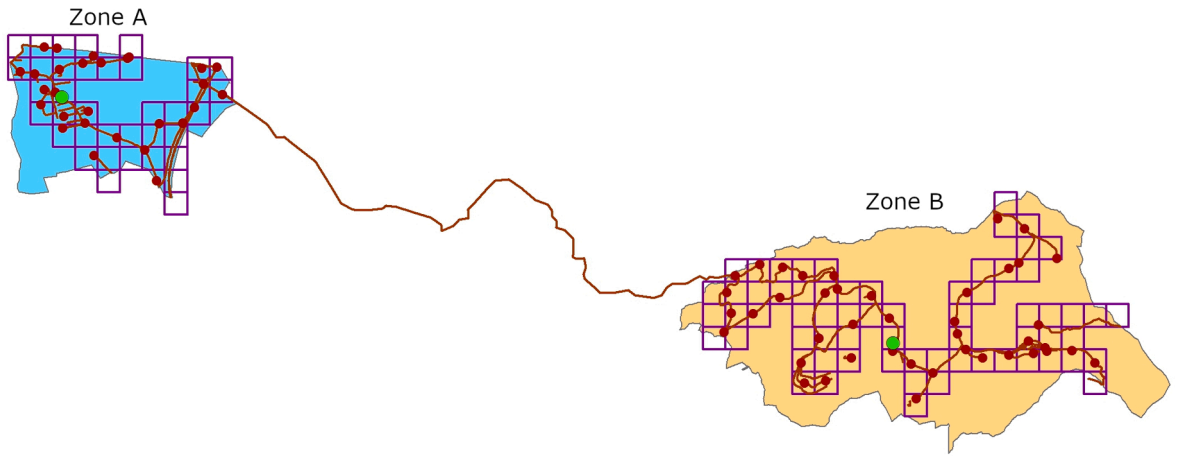

Fig. 6. Illustration of two traffic zones (A and B) for calculating the shortest travel time path. Green nodes indicate centroid starting and end points for the calculation. Grid of 200 m by 200 m cells in two different traffic zones, red nodes selected for each cell along the road network, which are the basis for the calculation of average shortest travel time.

shortest travel time was calculated between the considered zones.

In the last step, average shortest travel time paths were identified between traffic zones under both normal conditions and during extreme flood events by considering all roads as possible detour options while travelling by car.

2.3.2. Population weighted Hansen index (A1)

We did not further investigate the normalized Hansen integral index measure (Eq. (1)) because it focuses on only opportunities in other zones beyond those in the source or original zone of interest. Thus, flood impact on the zone of interest has no effect on the accessibility-based vulnerability of the road network. Therefore, we modified the population weighted Hansen index (Eq. (3)) by the total number of opportunities available in the study area, except for opportunities in zone *i*. We consider the total number of employment places and schools (including primary and secondary level locations) together to represent opportunities, as exemplified in Chen et al. (2015). Additionally, the population of zone *i* was also normalized by the total population of the study area. We call this modified approach A1 (or A_{out}). The equation becomes:

$$A1_i = \frac{P_i}{P_{total}} \times \frac{\sum_j B_j f(C_{ij})}{\sum_j B_j}, \tag{7}$$

where B_j is the total number of opportunities in a given traffic zone, which is the combination of employment and school places.

$$B_j = Emp_j + Sch_j. \tag{8}$$

Emp_j – employment places in traffic zone *j*
Sch_j – schools in traffic zone *j*

The population weighted Hansen index (A1, (Eq. (7))) identify how residents of the traffic zone of interest (or the source area) take part in particular activities (e.g., work and study) in other zones. Therefore, attractiveness between traffic zones is defined by both the population living in the source traffic zone and the availability of opportunities in other zones.

2.3.3. Opportunity weighted accessibility index (A2)

Similar to the modified population weighted Hansen index (Eq. (7)), Chen et al. (2015) used employment and school places as an attraction weight (Eq. (9)) but normalized opportunity and population are swapped in their positions. That implicates how opportunities in the traffic zone of interest is attracting the population of other traffic zones with respect to overall accessibility.

$$A_i = \frac{B_i}{B_{total}} * \sum_j^{n-1} \frac{P_j}{P_{total}} f(C_{ij}) \tag{9}$$

$$B_i = Emp_i + Sch_i. \tag{10}$$

$\frac{B_i}{B_{total}}$ – attraction weight of zone *i* (i.e., employment and school enrolment weight of zone *i*, which equals ratio of employment and school enrolment in zone *i* to the total employment and school enrolment in the whole study area);

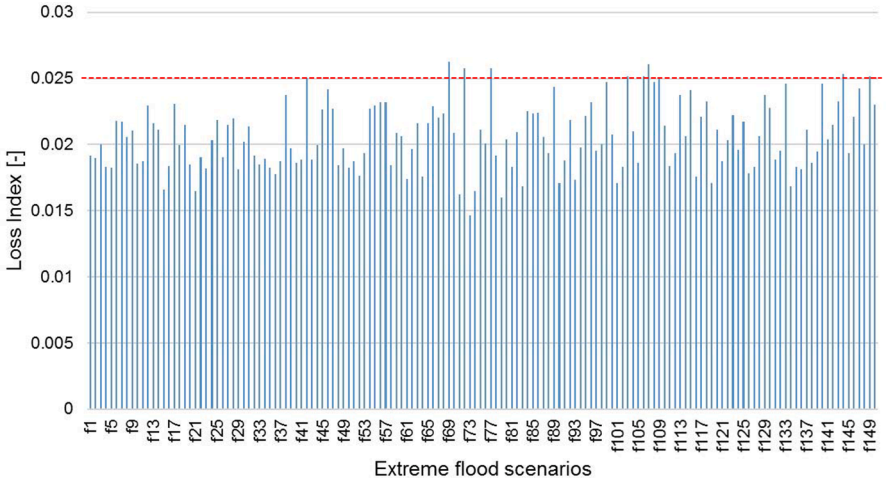

Fig. 7. Loss Index of flooded roads (greater than0.2 m) identified from 150 probable maximum flood scenarios in the considered Aare River basin. Flood scenarios are noted in the x-axis from f1 to f150. Red line indicates a threshold of 0.025, which means more than 2.5% of the road surface in the study area are flooded.

$\frac{P_j}{P_{total}}$ – weight of population in zone *j*, which equals the ratio of population in zone *j* to the entire population in the whole study area.

Considering this background, (Eq. (9)) can be rewritten as A2 (A_{in}):

$$A2_i = \frac{Emp_i + Sch_i}{Emp_{total} + Sch_{total}} * \sum_{j}^{n-1} \frac{P_j}{P_{total}} f(C_{ij}) \tag{11}$$

The opportunity weighted accessibility index (A2, (Eq. (11))) shows how residential populations of other traffic zones are attracted to opportunities present in the source zone.

2.3.4. *Transport, opportunity, and population specific accessibility (TOPS-A)*

During the occurrence of a flood event, we consider both changes (i) to the flood-affected population as well as opportunities and (ii) average travel times in the accessibility measure. Calculation of accessibility during a flood for each traffic zone includes populations and opportunities outside of the flooded areas. We adapt the presented approaches to address flood impact accordingly.

The modified population weighted Hansen index (A1) during a flood is expressed as:

$$TOPS - A1_i = \frac{(P_i - P_{i\_flood\_hit})}{P_{total}} \times \frac{\sum_j (B_j - B_{j_{flood_{hit}}}) f(c_{ij})}{\sum_j B_j}. \tag{12}$$

The modified opportunity weighted accessibility index (A2) during flood is expressed as:

$$TOPS - A2_i = \frac{(B_i - B_{i\_flood\_hit})}{B_{total}} * \sum_{j}^{n-1} \frac{(P_j - P_{j_{flood_{hit}}})}{P_{total}} f(c_{ij}) \tag{13}$$

2.3.5. *Comparison between selected floods based on accessibilities*

Total accessibility is calculated by summing one type of accessibility (either A1, A2, TOPS-A1 or TOPS-A2) of 531 traffic zones before and during floods. The ratio of total accessibility is a relative, unitless measure, where total accessibility during flooded conditions is divided by the total accessibility during pre-flooded conditions. This measure also applies to overall vulnerability and enables the comparison of vulnerability under different flood scenarios. Besides calculating total accessibility, we also measure the average of accessibilities of 531 traffic zones prior to and during flood occurrences. In addition, a ratio of average accessibility is calculated by dividing the average accessibility during flood occurrences to the average accessibility associated with pre-flood conditions.

2.4. *Vulnerability indices and influencing factors*

We use relative values of the four outlined accessibility indices as vulnerability values, which indicate to which degree accessibility is reduced during flood occurrence, compared to the pre-flood conditions. To visualize vulnerabilities per traffic zone, defined interval classes which are similar to equal range classes used by Noland et al. (2019) are used, in particular, 0.2 for the ratio of accessibility.

Correlation analysis is carried out between vulnerability indices and population, and opportunities parameters to identify the relative degrees of influence. Additionally, we use geographic maps with 531 traffic zone, where each zone has an assigned

Table 2
Flood scenarios selected by ranking of LI, Total-EBC, and Mean-EBC to measure flood impact on the road network and divergent ranking between the approaches.

Criteria	Loss Index	Total-EBC	Mean-EBC	Difference (Mean-EBC – Total-EBC)	Flood scenario
Maximum by LI	**1**	6	14	8	f69
Maximum by Total-EBC	4	**1**	3	2	f77
Maximum by Mean-EBC	16	15	**1**	-14	f147
The highest negative difference	149	149	28	**-121**	f79
Maximum difference	12	3	148	**145**	f108

Table 3
Key information for selected flood scenarios including information on the selection criteria (see Table 2). Total road surface = 27,361,108 m^2; Total road length = 6,703,328 m. Highest values are marked in bold.

Flood scenario	f69 (LI)	f77 (Total-EBC)	f147 (Mean-EBC)	f79 (Diff. negative)	f108 (Diff. positive)
Total flooded area (m^2)	**27,750,000**	27,450,000	25,352,500	19,945,000	27,722,500
Total flooded road surface (m^2)	531,758	530,702	460,203	255,092	**539,205**
Total flooded road surface (m^2)/Total road surface (m^2)	0.0192	0.0193	0.0168	0.0093	**0.0197**
Total flooded road length (m)	111,126	**112,726**	100,166	55,905	112,214
Flooded major roads (m)/Total flooded road length (m)	0.237	0.228	0.214	0.193	**0.238**
Road area (m^2) only flooded by one specific scenario	2,122	8,038	0	52	**77,604**
Number of affected TZs (with flooded road surface) and ratio to overall TZs	**96** **0.18**	**96** **0.18**	94 0.177	82 0.15	90 0.17
Number of affected TZs, only affected by one specific scenario	6	14	0	1	**40**

vulnerability value to represent the regional effects on total vulnerability indices. Linear regression analysis is applied to identify the relationship between changes in accessibility values in each traffic zone based on TOPS-A1 and TOPS A2 approaches to changes in travel time, population, and opportunities due to the impact of each flood scenario.

3. Results and discussions

3.1. Measure for flood impact and selection of extreme flood scenarios

Fig. 7 shows the distribution of the Loss Index (LI) for 150 flood scenarios. Only one scenario generates a LI below 0.015 and thus directly affects just 1.5% of road areas or surfaces out of the 150 flood scenarios considered. Sixty-seven scenarios resulted in LIs between 0.015 and 0.2, and 73 scenarios with LIs between 0.02 and 0.025. The nine most extreme floods identified by this measure reach or exceed an LI of 0.025 (above the red dotted line in Fig. 7), which covers more than 2.5% of the road area in study regions.

The rankings of flood scenarios based on LI, Total-EBC, and Mean-EBC are presented in Table A.2, as is the difference between Mean-EBC and Total-EBC. The relationship between LI and Total-EBC (see Fig. A.1) is monotonic and strongly positive. Spearman's correlation coefficient between the LI and the Total-EBC is 0.97 and is statistically significant ($p = 0$).

A range of flood scenarios were then selected for further analysis based on the ranked evaluation criteria. For instance, flood scenario f69 is ranked highest among all flood scenarios for the LI value (see Table 2 and Table A.2), representing the highest proportion of inundated road surface area. However, flood scenarios f77 and f147 are highest ranked for Total-EBC and Mean-EBC values, respectively. Due to the high correlation between LI and Total-EBC (Fig. A.1 and examples in Table 2), only Total-EBC is compared with Mean-EBC. Flood scenarios f79 and f108 were identified as representing the most pronounced differences in both negative and positive values (see Table 2 and Table A.2). Flood scenario f79 represents a lower direct impact to the road network with the second-lowest LI and Total-EBC values. In contrast, flood scenario f108 represents a higher direct impact to the road network but is ranked third for Total-EBC. Moreover, scenario f77 was also similarly ranked across all three measures, whereas rankings shift from f69 to f147 between LI and Mean-EBC values (see Table 2).

3.2. Comparison of selected flood scenarios by direct impacts

Table 3 presents an initial overview of the selected flood scenarios' key characteristics in flooded areas, affected roads, and Traffic Zones (TZ).

Flood scenarios f69 and f77 share highly similar total flooded area, total flooded road surface, and number of affected TZs. However, differences arise in the number of affected TZs, and the road area is flooded by only one specific scenario. The f147 scenario affected slightly smaller areas than scenarios f69 and f77 but affected a similar number of TZs. Flood scenario f79 shows the lowest values for all the characteristics considered. Although flood scenario f108 shares comparable values with f69, f108 is based on a very different flood pattern characterized by the most extensive road area and TZs only flooded by this specific scenario. However, f108 affected fewer TZs than scenarios f69, f77, and f147.

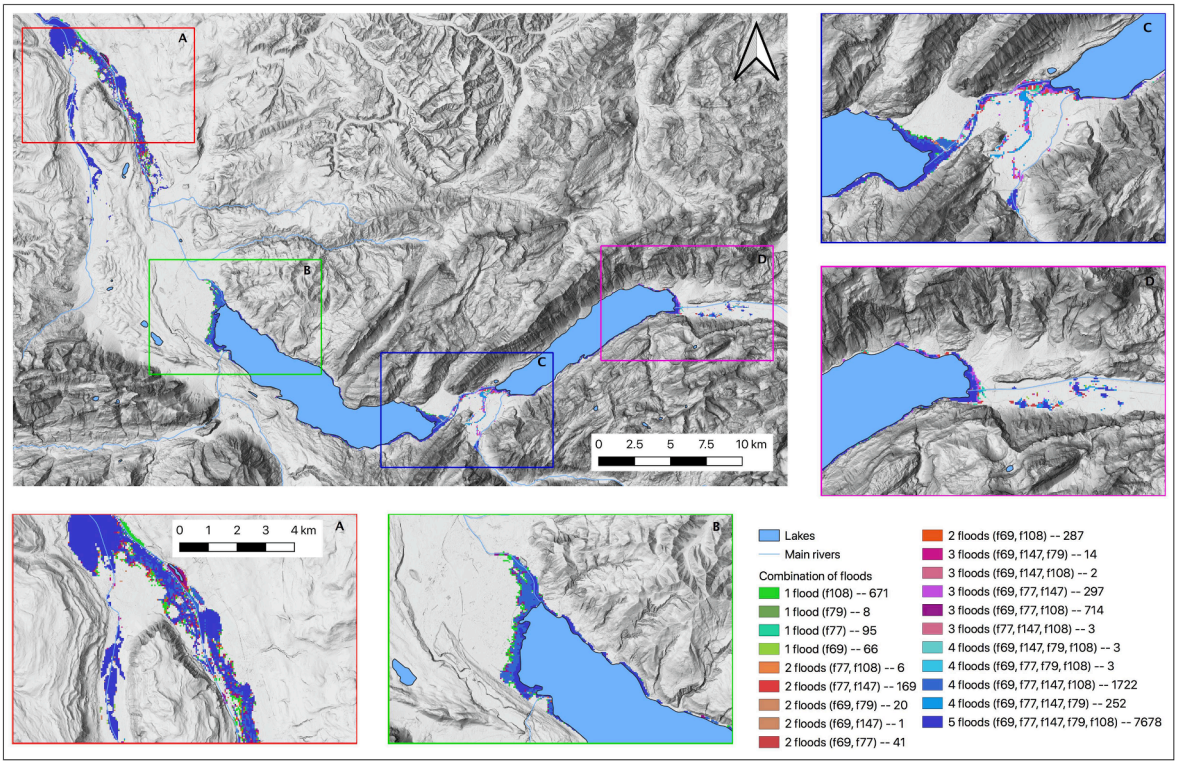

Fig. 8. Flooded areas of selected scenarios in the study area. Flood scenarios are overlaid to indicate areas which are flooded in several scenarios (3–5 flood scenarios) and which are only affected by specific flood scenarios (1–2 flood scenarios). Numbers after flood combinations (such as - - 671) indicate number of pixels of 50 m by 50 m. Four zoom-in areas provide a more detailed overview of the most affected regions.

Table A.3. shows that the selected flood scenarios affect 84 traffic zones, and most of the traffic zones are affected by three to five flood scenarios. Additionally, the geographic extent of the extreme flood scenarios is compared, based on common flooded areas under various combined flood scenarios. Each combination is differentiated by colour in Fig. 8. Four main flooded areas (noted as A, B, C and D) are also enlarged to demonstrate which flood combination dominates in these areas. For all of these areas, the combination of five floods in blue is dominant or clearly covering a significant amount of area.

Because f108 has a different flood pattern from the other selected scenarios, we compare flood scenarios f79 and f108 in more detail over four sub-areas in Fig. 9.

Fig. 9A presents a good example of the differing flood extents of scenarios f79 and f108. Furthermore, different patterns are observed on flood-affected roads in the eastern part. Fig. 9B indicates that generally, the flood extent and the proportion of flooded roads near Thun is smaller or less in scenario f79 than in f108. However, f79 impacts more roads and more critical ones within the network, such as the motorway in Interlaken (Fig. 9C), than does f108. In f108, although a larger extent along the shore of Lake Thun is flooded, these affected areas consist of less critical road sections. In the Bernese Oberland (Fig. 9D), the main roads follow the lake shore and the Aare River. These are identified as key water sources and are directly affected when water levels rise during extreme events.

The pattern of direct impacts of extreme floods on the road network depends on the spatial pattern of floods. Both f79 and f108 could represent a group of flood scenarios with similar patterns and spatial extents. However, f79 and f108 differ greatly in direct flood impact.

3.3. Comparison of selected flood scenarios and applied approaches: indirect impacts

3.3.1. Accessibility-based vulnerability at a regional level

We use total and average accessibility indices to assess overall accessibility in the region. Firstly, we present total accessibility for all 531 traffic zones in the study area, both before and during flood conditions using four accessibility indices. Although interpretations of the four indices differ, the total accessibility identified for the whole study area under these two conditions has similar values when A1/A2 and TOPS-A1/TOPS-A2 approaches are applied (Table 4). Total accessibility before flood onset for all 531 traffic zones is 3193, a value that decreases during flood occurrence.

Table 4 shows that scenario f77 affects total accessibility the most, followed by f147, considering results from all four indices. In contrast, f79 produces the lowest accessibility impact of all flood scenarios. The different accessibility indices show the same patterns

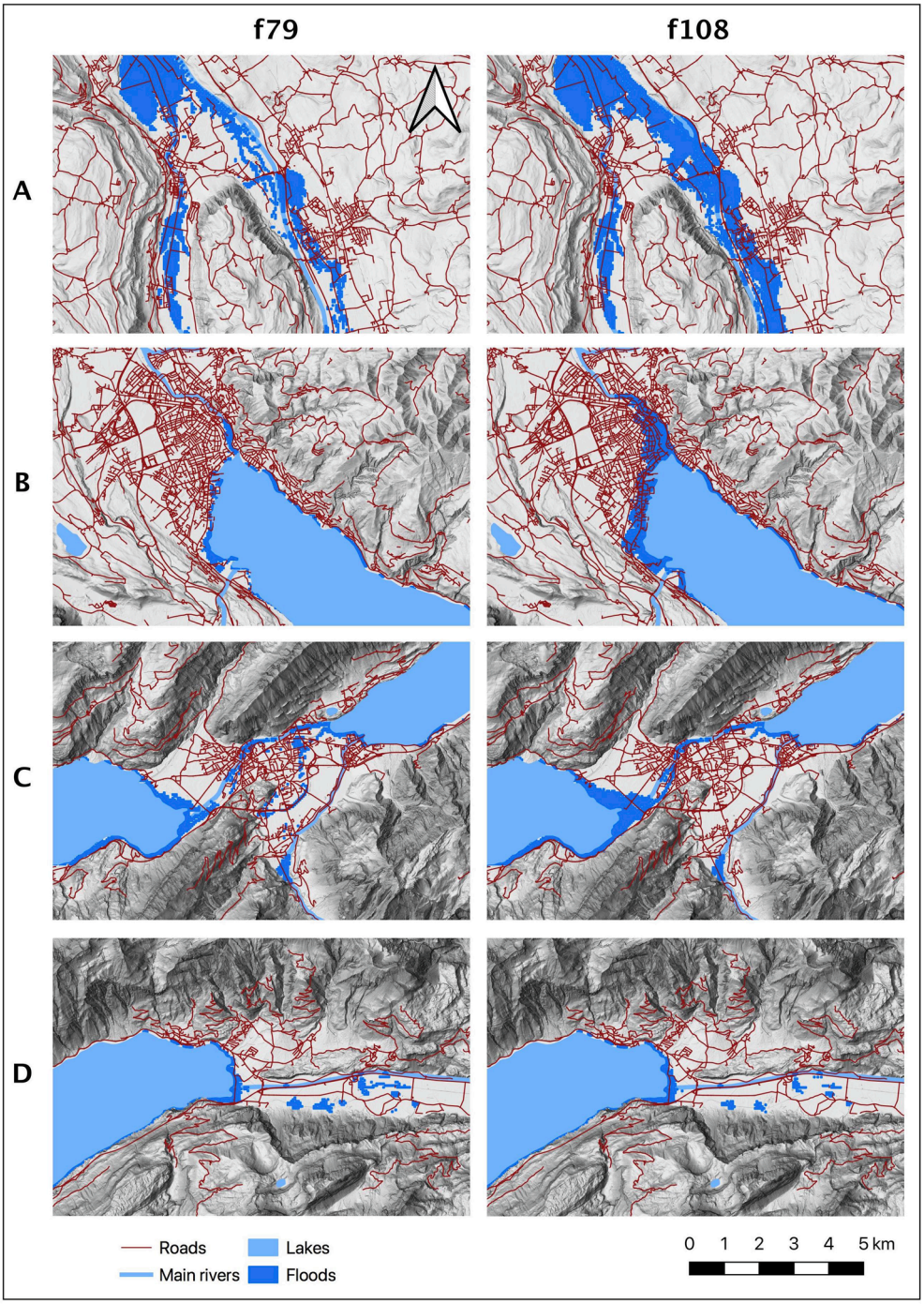

Fig. 9. Comparison of the effect on flooded roads by two flood scenarios, f79 (low rank of Total-EBC, high rank of Mean-EBC) and f108 (high rank of Total-EBC, low rank of Mean-EBC), presented in the zoom-in areas (A-D) of Fig. 8.

of impact for the selected flood scenarios. Flood scenario f77 is associated with the highest Total-EBC for flood-affected roads (Table 2), the greatest flooded road length, and the highest number of affected TZs (Table 3). Thus, accessibility indices calculated for f77 also indicate the lowest total accessibility (Table 4). Overall, TOPS-A1 (TOPS-A2) ratios function as indicators of vulnerable areas, where lower accessibility is observed than for the ratios of A1 (A2) before and during flood events.

Secondly, average accessibility in the study area before flood occurrence is 6.01 for A1 and A2. Average accessibilities during floods and ratios between average accessibilities during and before flood conditions are listed in Table 5.

The ratio of average accessibilities listed in Table 5 also identifies f77 as having the lowest overall average accessibility during

Table 4
Total accessibility based on four accessibility indices in various flood scenarios and ratio of changes, compared with values without flood impact (value 3193). Values indicating most notable changes are in bold.

Flood scenario/indices	A1 (A2) during floods	Ratio (A1/3193)	TOPS-A1 (TOPS-A2) during floods	Ratio (TOPS-A1/3193)
f69	2776	0.87	2718	0.85
f77	2748	**0.86**	2697	**0.84**
f147	2769	0.87	2732	0.85
f79	2878	0.90	2859	0.89
f108	2787	0.87	2735	0.86

Table 5
Average accessibility indices during flood scenarios and ratio of changes compared to values without flood impact. Values with strongest change are in bold.

Flood scenario/indices	Total average A1/A2 during floods	Ratio of change	Total average TOPS-A1/TOPS-A2 during floods	Ratio of change
f69	5.22	0.87	5.12	0.85
f77	5.17	**0.86**	5.08	**0.845**
f147	5.21	0.87	5.15	0.86
f79	5.42	0.90	5.38	0.895
f108	5.25	0.87	5.15	0.857

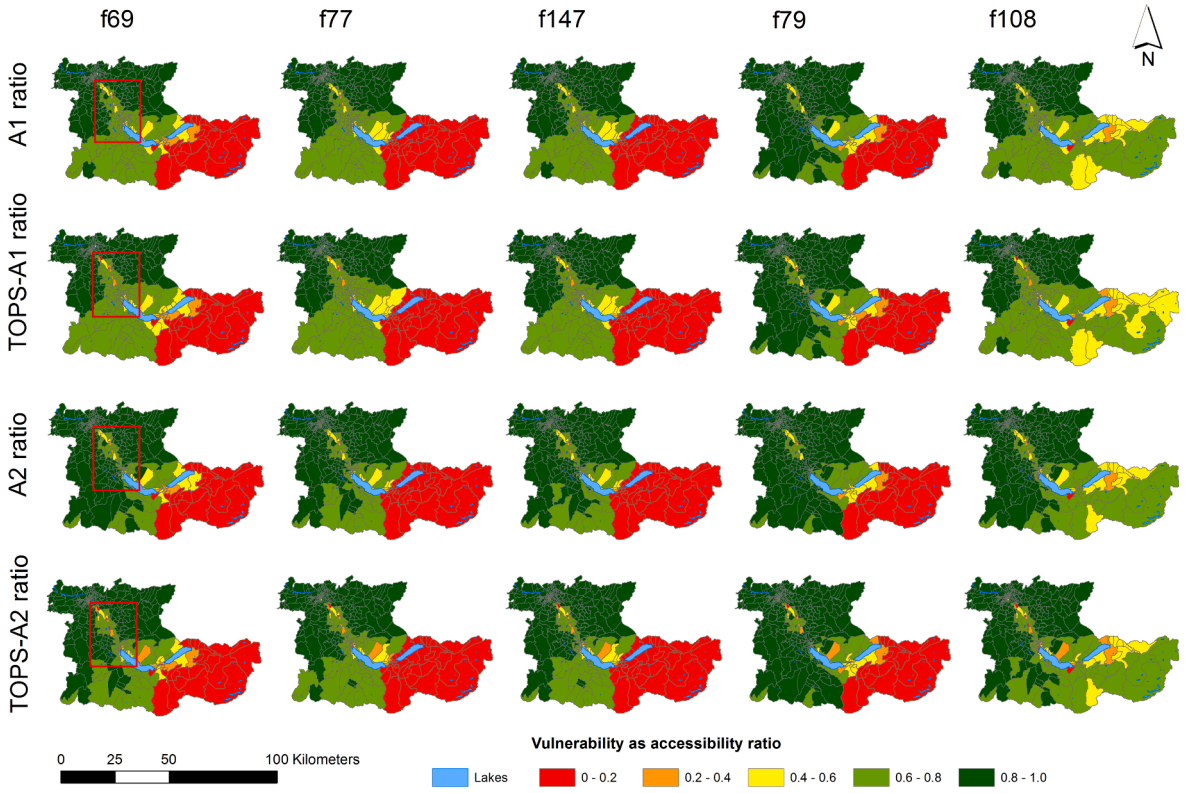

Fig. 10. Vulnerability as an accessibility ratio calculated with A1 ratio, TOPS-A1 ratio, A2 ratio, and TOPS-A2 ratio (top to bottom). The first column of results corresponds to flood scenario f69, followed by results of flood scenarios f77, f147, f79 and f108, respectively (left to right).

floods. In contrast, f79 was consistently identified as having the highest accessibility of all flood scenarios. Both total (Table 4) and average accessibility indices (Table 5) indicate values that are up to 2% lower for TOPS-A1 and TOPS-A2 indices than those for A1 and A2 indices.

3.3.2. Spatial pattern of vulnerability based on traffic zones

Because vulnerability is defined as a ratio of accessibility between before and during floods (Section 2.4), the spatial pattern of

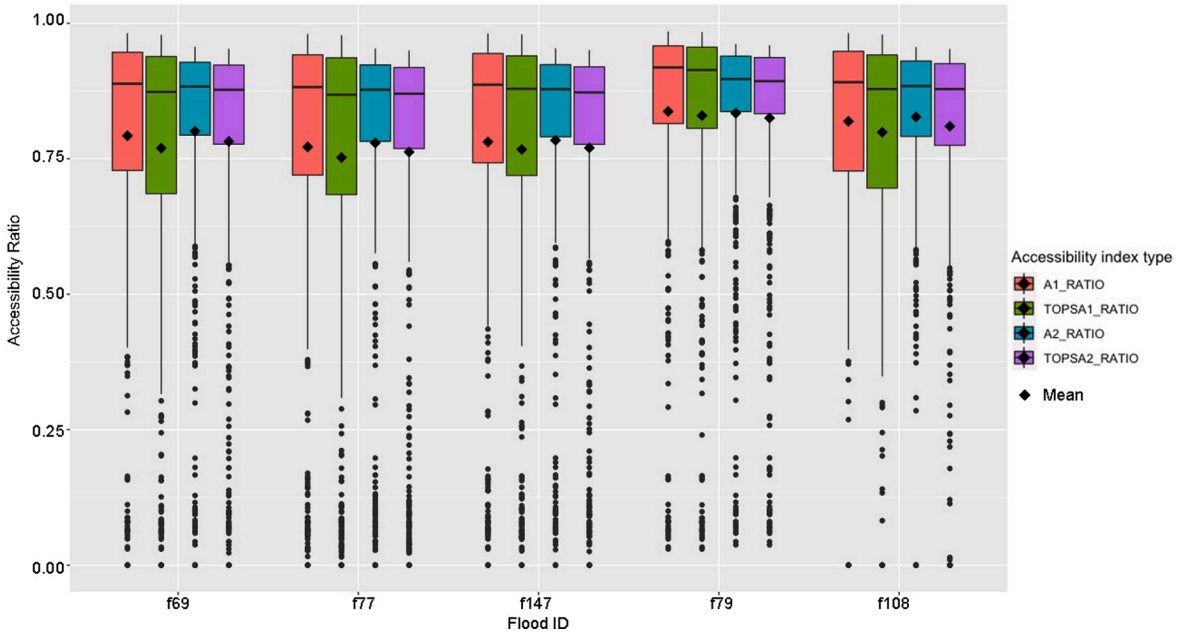

Fig. 11. Boxplots of ratios of accessibility indices A1, TOPS-A1, A2, TOPS-A2 in different flood scenarios. Mean values are indicated in diamond shaped points.

vulnerability in various flood scenarios is investigated. The vulnerability results for four approaches and calculated for five flood scenarios are illustrated for all 531 traffic zones (TZs) in Fig. 10. The most vulnerable TZs with the lowest accessibility ratios are presented in red. Fig. 10 highlights differences among flood impacts organized by TZs. However, all selected flood scenarios show a similar regional pattern, where most TZs in the central and eastern parts of the study area have lower accessibility ratios than those in the northern part, even though TZs along the floodplain between Thun and Bern are characterised by two low impact zones (dark and light green classes) in various flood scenarios.

In Fig. 10, vulnerabilities of individual zones have somewhat similar patterns in the f69, f77, f147, and f79 flood scenarios. These patterns highlight traffic zones with accessibility ratios less than 0.2, especially in the south-eastern corner of the study area. In contrast, vulnerabilities of individual zones in f108 differ where there are only a few traffic zones with accessibility ratios of less than 0.6.

The results show differences between the weighted Hansen index (A1 or A2) and the modified Hansen index (TOPS-A1 or TOPS-A2) are particularly significant for neighbouring areas of flood-affected traffic zones. In particular, TOPS-A2 highlights an increase in vulnerability in the neighbouring TZs and a slight increase of vulnerability in some more distant TZs.

A spatial zoom-in presented in Fig. A.4 (areas indicated as red rectangle in Fig. 10) of flood scenario f69 highlights ratio change differences for each approach per traffic zone. The A1 and TOPS-A1 approaches have a spatially wider impact than the A2 and TOPS-A2. This difference is attributed to differences in population distributions, densities, and opportunities. The spatial spread of affected TZs increases when comparing A1 to TOPS-A1 and A2 to TOPS-A2, because flood-affected populations and opportunities are incorporated in TOPS-A1 and TOPS-A2. This suggests an improvement in the accuracy of the accessibility calculation with the spatially aware TOPS approaches, thereby improving the accuracy of vulnerability calculations in these individual traffic zones. The spatial effect on accessibility of choosing either a population-weighted or an opportunity-weighted approach is clearly illustrated in Fig. 10 and Fig. A.4.

3.3.3. Statistics of vulnerability

To gain insights into the effects of different approaches, we compare the vulnerability of individual traffic zones under different flood scenarios by generating box plots of the ratios of each accessibility index. Statistics on the ratios of all accessibility indices computed under five flood scenarios for 531 traffic zones are illustrated in Fig. 11. Fig. 11 shows the effects of flooding in A1 and A2 indices are comparable for each flood, as are the effects of TOPS-A1 and TOPS-A2. However, mean ratios of TOPS-A1 and TOPS-A2 are up to two percentage points lower than mean ratios of A1 and A2 indices per flood.

Scenario f79 is associated with the highest ratio values (maximum, median, and mean) among the flood scenarios, but resulted in the smallest ranges of ratios. This suggests that scenario f79 resulted in the lowest vulnerability of road networks in the study area; this finding is consistent with key information about the flood scenario summarized in Table 3. Although mean ratios of A1 indices for f79 and f108 are similar (0.83 and 0.82, respectively) and higher than the ratios of the other three scenarios (Fig. 11), the range of ratios for f79 and f108 are distinctly different. Flood scenario f108 is associated with fewer outliers than f79, which means a higher number of TZs with reduced impact on accessibility during floods. Moreover, the range of ratios of the TZs for f108 shows a similar distribution as

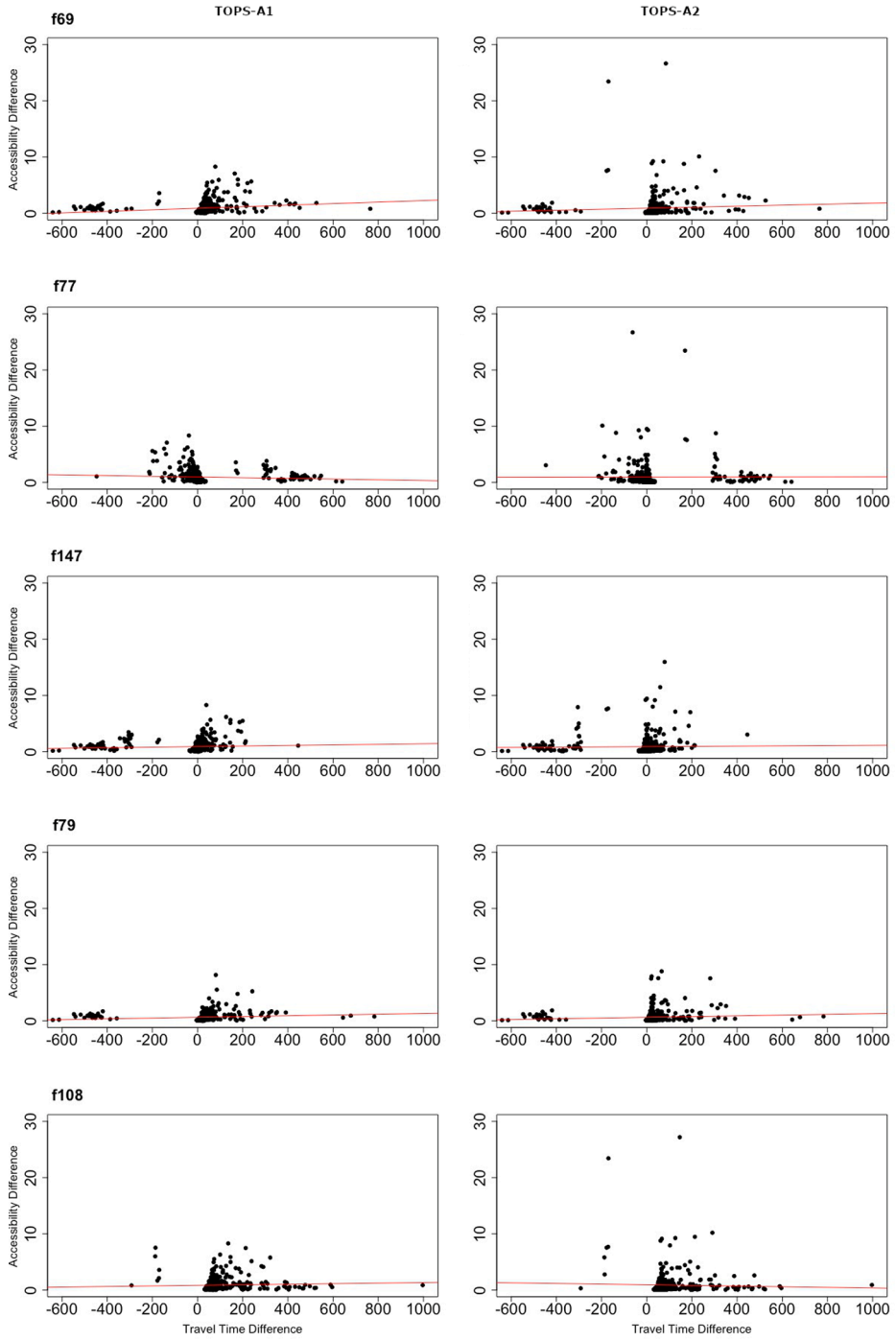

Fig. 12. Relation of changed travel time due to the impact of flooded roads and difference of accessibilities after floods based on TOPS-A1 and TOPS-A2 for the five selected flood scenarios (f69-f108).

those of f69 and f77; this also corresponds well with the key flood scenario information in Table 3. In contrast, the range of ratios for f79 contains a higher number of outliers, which indicates strong impacts on accessibility per TZ here, where the median is the highest of all scenarios. Flood scenario f147 has a smaller range of accessibility changes within the individual TZs than the ranges calculated for scenarios f69, f77, and f108.

In contrast to similar mean values obtained with A1 and A2 approaches (and also with TOPS-A1 and TOPS-A2), the median of the ratios under all of the scenarios using the TOPS-A1 and TOPS-A2 approaches are lower than those of A1 and A2 approaches. In addition, maximum and Q3 (75%) values of A2 and TOPS-A2 are consistently lower than those of A1 and TOPS-A1 approaches. These

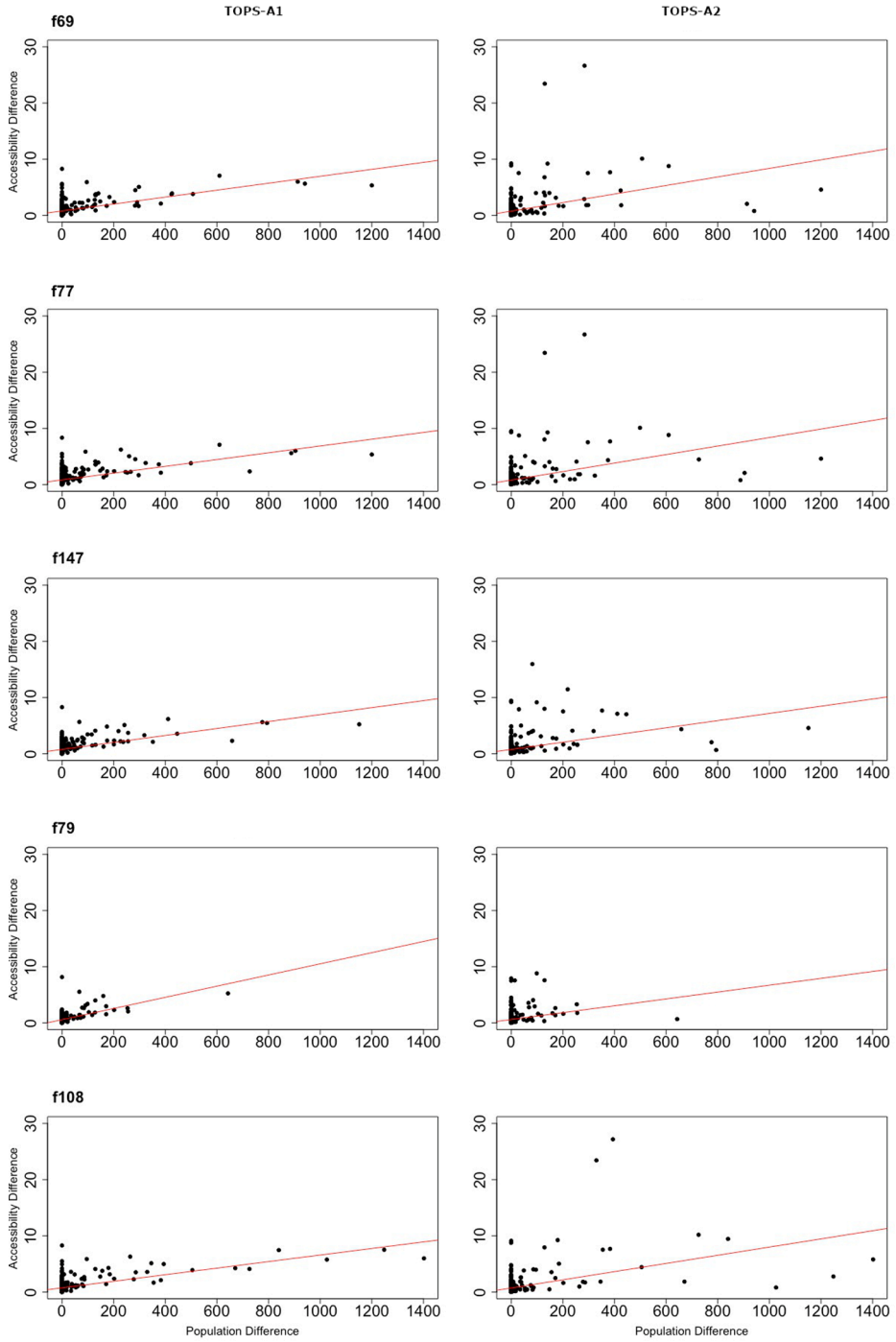

Fig. 13. Relation of changed population due to the impact of floods and difference of accessibilities after floods based on TOPS-A1 and TOPS-A2 for the five selected flood scenarios (f69-f108).

results indicate that ratios of opportunity-weighted accessibility approaches are generally lower than those of population-weighted accessibility approaches.

Because both A1 and A2 accessibility indices originated from the Hansen integral accessibility index, the results indicate both differences and similarities. The total accessibilities obtained with these approaches are comparable (Table 4), which is expected. However, accessibilities for individual traffic zones differ depending on the attractiveness factors: population for A1 and opportunities for A2. Correlations between population and A1 and between opportunities and A2 are verified prior to the onset of floods. As expected, the scatter plot in Fig. A.2 shows a monotonous relationship between population and A1, with a Spearman correlation

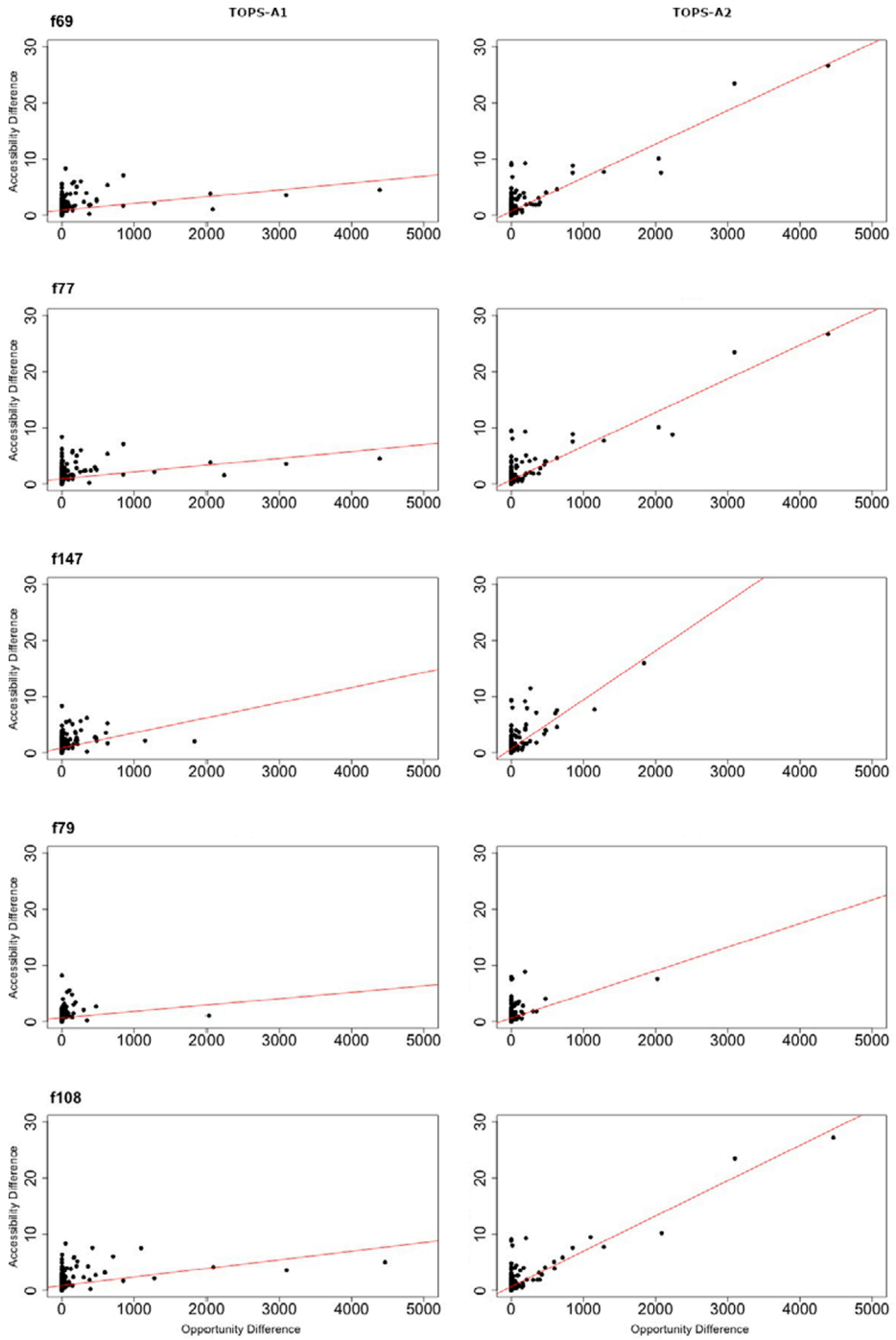

Fig. 14. Relation of changed opportunity due to the impact of floods and difference of accessibilities after floods with TOPS-A1 and TOPS-A2 for the five selected flood scenarios (f69-f108).

coefficient of 0.77 (Table A.4). Fig. A.3 shows a linear relationship between opportunities and A2, with a Pearson correlation coefficient of 0.91 (Table A.4). According to the definition of accessibility, when opportunity increases in the area, the accessibility to this area should also increase (Geurs and van Wee, 2004). The modified indices, TOPS-A1 and TOPS-A2, also follow this definition (see Fig. A.3).

3.4. Vulnerability and influencing factors

3.4.1. Statistics of influencing parameters for vulnerability

The results of the TOPS-A1 and TOPS-A2 approaches provide the strength of influence that contributing parameters such as travel time (Fig. 12), population (Fig. 13), and opportunities (Fig. 14) have on each flood scenario.

Fig. 12 explains how each flood scenario has different effects on travel time and accessibility indices. When TZs become partially accessible or completely inaccessible due to floods, travel times between these and other affected zones are reduced or become undefined, which is indicated by negative time differences. In general, Fig. 12 indicates a very weak (TOPS-A1) and a lacking (TOPS-A2) linear relationship between travel time changes and the overall change of accessibility prior to and during floods. What is noticeable is the spread of differences of accessibility values around 0 to +/- 100 hrs of travel time change. However, TOPS-A2 resulted in stronger differences in the accessibility values for four scenarios than with the use of TOPS-A1. Although the calculation for travel time between TZs uses the same method for both accessibility approaches, different TZs are affected depending on whether population or opportunities are used as weight factors.

Furthermore, the selected flood scenarios resulted in divergent numbers of TZs with negative and positive differences in travel time (Fig. 12). Under f108, the number of TZs with negative differences is lower than those identified in other flood scenarios, yet the number of TZs with positive differences in travel time is the highest, with values of up to 1000 hrs. The highest number of positive differences in travel time indicate that these TZs are all accessible but that the time needed to travel from one TZ to another increased. Even though several TZs have increased travel times, the difference in accessibility values between the pre-flood and flood situations remains low for this scenario. Thus, f108 results in the second most accessible road conditions, indicated by a 0.80 mean of ratios value when TOPS-A1 is applied (Fig. 11). In contrast to f108, f147 results in numerous TZs with high negative travel time differences, which indicates partially accessible routes in these zones but many TZs with positive values for differences of up to 450 hrs. Scenario f77 resulted in the highest number of TZs with negative travel time differences and highly variable accessibility. Because f77 resulted in the lowest mean of ratios among all scenarios evaluated with TOPS-A1 (Fig. 11), it is the scenario with the highest vulnerability. Table 3 shows that f79 has the lowest values of flood-affected TZs and roads. However, it has significantly higher negative travel time differences than f108. These higher differences are caused by flood disturbance of highly connected roads. Overall, accessibility difference depends weakly on travel time difference in the study area. However, it can be strongly dependent for some traffic zones in particular locations.

Fig. 13 focuses on the influence of population and indicates two clusters: first, f79 with the lowest accessibility differences in both approaches of TOPS-A1 and TOPS-A2, and second, the rest of the floods with higher accessibility differences in TOPS-A2 than TOPS-A1. As the proportion of the population affected rises, the differences of accessibility values also rise, but with a slightly different slope for f79 compared to the other flood scenarios in TOPS-A1. This pattern is related to the overall low proportion of population affected in f79. Despite the fact that some TZs have nearly none or only a small affected population, the accessibility values differ between the pre-flood and flood situation in these TZs. These effects hold for the results of both TOPS-A1 and TOPS-A2. One reason for this effect is the increases in travel times between these TZs and other TZs during floods.

Fig. 14 indicates the influence of the opportunity parameter, where three patterns are identified. First, f79 has the lowest differences in opportunity and the lowest accessibility differences for the most TZs. Second, f147 has a similar range of differences in opportunity to f79, but f79′s differences in opportunity and accessibilities are lower. Third, f69, f77, and f108 have high differences in opportunity and high differences in accessibility. These results show again that accessibility values for TZs with no or low changes of opportunities are influenced by changing travel time due to the effects of floods in other TZs. Similar patterns exist among the flood scenarios for TOPS-A2. As expected, differences in opportunities affect differences of accessibility in TOPS-A2 more linearly than in TOPS-A1.

The strength of influence between differences of accessibilities and differences of contributing parameters varies as flood scenarios change. Varying accessibility differences in TZs near zero and very low differences in population and opportunities are explained by the influence of travel time differences.

3.4.2. Spatial context for influencing parameters

The accessibility-based vulnerability approaches are influenced by changing travel times due to the distribution of flooded roads and the availability of detours. The application of the new approach, considering the average shortest travel time as well as all road types, allows the integration of a variety of pathways during the flood event. The overall results indicate the presence of a spatial effect defined by the overlap of flood extent and a limited number of road connections. In the south-eastern part of the study area, TZ vulnerabilities are higher than other zones' when evaluated for all selected flood scenarios (see Fig. 10). This is attributed to the influence of an increased travel times due to flooded roads. Furthermore, the spatial effect of vulnerability is present in many TZs when comparing the overall results; the spatially explicit results are visualised in Fig. 10. This characteristic is attributed to higher accessibility in traffic zones in the central part of the study area, such as in f79 (see Fig. 9B). Overall, f79 has lower direct impact fewer roads are affected and a high number of possible detours in the dense road network. Nevertheless, f79 engenders higher indirect impact or vulnerability in remote areas due to inaccessibility or lower accessibility, especially near Interlaken (see Fig. 9C). This exemplifies how flood effects differ on local and regional scales and on specific road networks.

Furthermore, spatial distributions of population and opportunity parameters within the vulnerability assessment exhibit different spatial effects. Traffic zones near Thun have both high densities of population and opportunities. In contrast, TZs near Meiringen are the least populated and have the fewest opportunities (see Fig. 2). Vulnerabilities of TZs near Thun under scenario f79 are very low due to high accessibility ratio compared to other scenarios (fourth column of Fig. 10). This is because only a small proportion of the

population and opportunities of these zones are affected. Furthermore, the impacts are offset by the presence of a dense local road network. Even though population and opportunities are least affected in and near Meiringen, all TZs are affected by increased travel time because floods that occur near Interlaken, 30 km away, disrupt the highly connected roads.

3.5. General discussion

Direct impact of extreme floods to the road network: We extended the use of Mean-EBC together with Total-EBC in divergent ranking criteria to select individual flood scenarios among 150 extreme events with different impact patterns. Previously, Kermanshah and Derrible (2017) concluded that the impact of any extreme flood should be investigated alone, after demonstrating how to quantify the impact of extreme floods using mean edge betweenness centrality in two cities. Although this statement is true when investigating different areas, divergent ranking criteria could be used to compare multiple extreme floods in the same area. The divergent ranking difference appears to be a quick and efficient method to select for flood scenarios with contrasting direct impacts caused by different spatial patterns. Thus, it also supports the grouping of extreme floods with characteristic impact patterns. By doing so, it is assumed that flood scenarios in the same group having similar spatial patterns that can result in similar vulnerability patterns in a given region.

Furthermore, our results present the use of Mean-EBC in a larger region with different local road network configurations compared to the analysis of a road network in a single city (Casali and Heinimann, 2019b). Since our study area consists of different urban and rural areas, the results show how accessibility-based vulnerability is dependent on road connectivity between these areas.

More information about the local road network: We incorporated possible detours by considering the most detailed local roads in the accessibility analysis under flooded conditions. In previous studies, the shortest travel time path was only computed with major roads connecting the centre of the census area to emergency facilities (Gori et al., 2020) and from city to city (Taylor et al., 2006) are used. As an extension of this analysis, we use the average shortest travel time path between traffic zones to account for all possibilities from each node in one zone to all other nodes in another zone. Despite the higher computation required, the extended analysis we conducted ensured that the average shortest travel time produces the most realistic impedance value in the accessibility results.

Including additional parameter in the vulnerability analysis: The accuracy of vulnerability analysis of traffic zones to extreme floods is increased when the calculation accounts for flood affected populations and opportunities. Results demonstrate that although the average vulnerability difference in the region is between 1% and 2%, the vulnerability of individual traffic zones shows a more precise and accurate outcome. Therefore, including the additional parameter in the accessibility calculation is found to improve the vulnerability analysis at the regional scale. Unlike previous study by Taylor and Susiliwati (2012), where the vulnerability of only rural areas were assessed using an accessibility measure, our study applies the accessibility to the vulnerability assessment of a region, which includes urban, *peri*-urban and rural areas in the study area.

Moreover, comparison of different accessibilities with flood affected population and opportunities at a regional scale fills a gap. In particular, we gain insight about which vulnerability approach is suited to assess spatial socio-economic impacts, as suggested by Caschili et al. (2015). However, our current study is limited to accounting for population and opportunities due to data availability. Including time-dependent variables such as travel time and traffic volume data in the accessibility assessment would generate more realistic results. This promising research avenue for future studies depends on the availability of suitable data.

Identifying the vulnerable traffic zones and comparing the different approaches: Results indicate not only the most vulnerable traffic zones under one flood scenario but also the most vulnerable traffic zones for the majority of the flood situations. Specifically, the traffic zones in the south-east are the most vulnerable due to disturbances to the highly connected roads that serve these zones. Compared to the findings in Kermanshah et al. (2017), our study identifies traffic zones that have similarly high vulnerability under different extreme flood scenarios.

Overall, compared to the ratios of A1 (A2) before and during floods, the ratios of TOPS-A1 (TOPS-A2) identify vulnerable areas more precisely because they account for flood-affected population and opportunities. For each TZ, the interpretation of accessibility measures A1 and A2 is different. Since TOPS-A1 and TOPS-A2 originated from the A1 and A2 respectively, interpretations of TOPS-A1 and TOPS-A2 follow those of A1 and A2 but with increased precision.

4. Conclusions

The main objective of this study was to compare different methods to assess direct and indirect impacts of extreme floods to road networks at regional scales. To quickly gain an overview of direct impacts, we used three effective measures, namely Loss Index, Total-EBC, and Mean-EBC. Furthermore, we extended the use of EBC by adding the divergent rank measure between Mean-EBC and Total-EBC for road networks affected by different flood scenarios. The divergent rank measure supported the selection of representative flood scenarios with different patterns in terms of geographical extent and network topology. Overall results highlighted that different types of flood scenarios with their distinctive impact patterns correspond with patterns of vulnerability based on accessibility.

In the accessibility analysis, we used average shortest travel time path between traffic zones considering flood affected areas, instead of the shortest travel time between centres of traffic zones. This method identifies more realistic travel paths and consequently travel time during the occurrence of extreme floods.

The most vulnerable traffic zones were identified for each of the selected extreme flood scenarios using the population-weighted Hansen index (A1) and the opportunity-weighted Hansen index (A2), as well as the modified accessibility measures TOPS-A1 and TOPS-A2 to incorporate the influence of flood-affected populations and opportunities. The newly proposed accessibility measures TOPS-A1 and TOPS-A2 follow the general behaviour of accessibility measures, A1 and A2. The strength of influence on the accessibilities before and during the flood depends on the considered parameters (travel time, population, opportunities) used in the different

vulnerability approaches. Changes of travel time during the flood have less influence on the vulnerability results considering the directly affected traffic zone but indicate a more indirect influence if road sections of high connectivity are flooded. The influence of the differences of populations or opportunities during the flood on the vulnerability results are dependent on the different patterns of each flood scenario and on the spatial distribution of the parameters in the study area. Overall, TOPS-A1 is influenced by population and TOPS-A2 is strongly dependent on opportunities. Therefore, the use of these modified approaches to explicitly include flood-affected populations and opportunities was found to improve the accuracy of accessibility assessments of flood scenarios at the traffic zone level. Moreover, the results indicate a 1–2% higher difference of vulnerability on a regional scale compared to the measures of A1 and A2, but a much higher diversity in the individual traffic zones that are affected.

The comparative study of four different vulnerability approaches related to flood impact on the road network shows three important results: (i) the strong dependency of weighted parameters in the approaches, (ii) the different vulnerability results related to the aggregation level (overall study area vs traffic zones therein) and (iii) the effects of different flood scenarios with their direct, and more importantly, indirect impacts due the spatial distribution of the road network and the different connectivity levels of affected road sections. Therefore, flood protection work, planning and construction of detour routes should be carried out in these high connectivity road segments that are associated with relatively higher vulnerabilities. Since our analysis was carried out without traffic congestion information, the incorporation of travel time and traffic flow information in future work on accessibility-based vulnerability due to flood disruptions is recommended.

CRediT authorship contribution statement

Tsolmongerel Papilloud: Conceptualization, Methodology, Software, Formal analysis, Visualization, Writing – original draft, Writing – review & editing. **Margreth Keiler:** Supervision, Conceptualization, Visualization, Writing – review & editing.

Declaration of Competing Interest

The authors declare that they have no known competing financial interests or personal relationships that could have appeared to influence the work reported in this paper.

Acknowledgement

We thank Andreas Zischg and collaborators for making their atmospheric-hydro-hydraulic model output in Aare river basin available for this study.

Appendix

See Tables A.1–A.4 and Figs. A.1–A.4.

Table A1
Type of road in TLM road data set (Federal Office of Topography, 2019) and assigned weight as width.

Type of road in integer	Type of road in text	Weight as width [m]	Maximum speed allowed [km/hr] (depending on urban/rural area)
0	Motorway exit	8	60
1	Motorway entry	8	80
2	Motorway	12	120
4	Connection	8	50/80
5	Driveway	8	50/80
8	10 m street	10	50/80
9	6 m street	6	50/80
10	4 m street	4	50/80
11	3 m street	3	50/80
12	Place	8	50/80
20	8 m street	8	50/80
21	Motor street	12	50/80

Table A2
Ranking of flood scenarios by three measures and difference between two ranks in ascending order.

Flood scenario	Rank of LI	Rank of Total-EBC	Rank of Mean-EBC	Difference between Mean-EBC and Total-EBC
f79	149	149	28	-121
f62	88	127	9	-118
f138	113	138	23	-115
f81	122	137	24	-113
f41	104	134	26	-108
f83	143	143	36	-107
f37	110	135	29	-106
f4	126	125	33	-92
f30	78	100	10	-90
f44	83	124	41	-83
f34	103	122	43	-79
f97	90	108	30	-78
f124	89	101	25	-76
f88	96	112	39	-73
f87	73	79	8	-71
f104	64	76	6	-70
f21	147	146	77	-69

(*continued on next page*)

Table A2 (*continued*)

f59	66	72	5	-67
f58	119	107	44	-63
f90	141	140	79	-61
f49	87	91	32	-59
f94	85	85	27	-58
f111	120	117	59	-58
f53	94	90	35	-55
f20	116	103	52	-51
f64	136	133	82	-51
f82	65	60	12	-48
f76	79	81	34	-47
f39	86	89	42	-47
f23	130	129	83	-46
f18	84	82	38	-44
f125	50	50	11	-39
f11	111	102	65	-37
f73	150	150	114	-36
f19	56	53	18	-35
f29	132	116	81	-35
f127	123	123	88	-35
f24	77	74	40	-34
f40	114	113	80	-33
f71	148	148	115	-33
f74	146	147	117	-30
f148	80	75	46	-29
f98	81	78	49	-29
f63	53	48	22	-26
f5	129	121	95	-26
f25	47	44	19	-25
f3	82	80	55	-25
f15	145	145	121	-24
f119	142	142	120	-22
f134	144	141	119	-22
f129	19	28	7	-21
f93	139	139	118	-21
f101	140	144	123	-21
f22	101	94	75	-19
f132	91	83	66	-17
f26	100	106	89	-17
f85	39	31	15	-16
f141	74	63	47	-16
f116	137	131	116	-15
f147	16	15	1	-14
f146	43	29	16	-13
f75	59	62	50	-12
f139	92	104	92	-12

(*continued on next page*)

Table A2 (*continued*)

f48	118	111	99	-12
f61	138	136	124	-12
f52	135	132	122	-10
f51	108	95	86	-9
f106	6	11	4	-7
f9	63	61	54	-7
f8	72	68	62	-6
f107	2	7	2	-5
f60	70	66	61	-5
f122	76	71	67	-4
f1	97	109	105	-4
f128	71	56	53	-3
f36	134	130	127	-3
f42	9	19	17	-2
f68	38	23	21	-2
f112	93	86	85	-1
f78	98	92	91	-1
f99	11	20	20	0
f114	69	57	57	0
f126	133	128	128	0
f43	106	96	97	1
f77	4	1	3	2
f145	95	87	90	3
f136	131	126	129	3
f80	75	59	63	4
f72	3	8	13	5
f102	125	120	125	5
f7	49	65	72	7
f69	1	6	14	8
f135	124	118	126	8
f33	117	97	106	9
f70	67	58	69	11
f123	40	24	37	13
f31	58	73	87	14
f67	44	41	56	15
f32	99	84	100	16
f35	128	119	137	18
f47	34	43	64	21
f27	55	55	76	21
f10	115	110	131	21
f144	5	9	31	22
f46	17	22	45	23
f56	25	33	58	25
f16	121	115	140	25
f137	60	42	71	29
f50	127	114	143	29

(*continued on next page*)

Table A2 (*continued*)

f2	102	105	135	30
f113	20	17	48	31
f84	36	38	70	32
f105	112	98	130	32
f100	68	45	78	33
f120	61	39	73	34
f13	51	70	104	34
f140	13	14	51	37
f131	105	99	136	37
f110	57	69	107	38
f150	28	21	60	39
f57	26	35	74	39
f91	107	93	134	41
f121	109	88	132	44
f117	42	47	94	47
f130	32	36	84	48
f6	48	64	113	49
f133	14	18	68	50
f92	46	51	109	58
f45	35	40	101	61
f28	45	46	110	64
f14	62	77	141	64
f118	22	25	93	68
f17	27	32	103	71
f142	54	67	138	71
f54	33	37	111	74
f96	24	16	102	86
f95	41	54	145	91
f103	7	2	96	94
f89	15	4	98	94
f86	37	49	147	98
f65	52	52	150	98
f109	10	12	112	100
f149	8	5	108	103
f66	31	34	146	112
f143	23	26	139	113
f12	30	30	144	114
f55	29	27	142	115
f115	18	10	133	123
f38	21	13	149	136
f108	12	3	148	145

Table A3
Traffic zones affected by floods and their population and opportunity affected. No impact (0.000) or very high impacts of the parameters are indicated with the different colours.

		Population affected (%) by traffic zone					Opportunity affected (%) by traffic zone				
No	TZ_ID	f69	f77	f147	f79	f108	f69	f77	f147	f79	f108
1	35101054	0.000	0.000	0.000	0.000	0.000	0.030	0.000	0.000	0.000	0.030
2	35101055	0.149	0.149	0.104	0.104	0.190	0.048	0.048	0.048	0.048	0.051
3	35101066	0.053	0.050	0.037	0.037	0.053	0.142	0.124	0.088	0.088	0.142
4	35101071	0.109	0.109	0.109	0.109	0.109	0.004	0.004	0.004	0.004	0.004
5	35601002	0.004	0.004	0.004	0.004	0.004	0.024	0.024	0.024	0.024	0.024
6	35601005	0.000	0.000	0.000	0.000	0.000	0.015	0.000	0.000	0.000	0.022
7	57101001	0.001	0.001	0.001	0.001	0.001	0.004	0.004	0.004	0.004	0.004
8	57201001	0.081	0.206	0.189	0.056	0.052	0.034	0.041	0.041	0.028	0.021
9	57201002	0.000	0.006	0.006	0.001	0.001	0.000	0.000	0.000	0.000	0.000
10	57301001	0.012	0.055	0.020	0.000	0.000	0.201	0.218	0.218	0.137	0.148
11	57301002	0.000	0.008	0.000	0.000	0.000	0.138	0.244	0.244	0.000	0.127
12	57301003	0.049	0.049	0.049	0.025	0.015	0.077	0.070	0.070	0.034	0.036
13	57501001	0.000	0.099	0.074	0.025	0.125	0.000	0.000	0.000	0.000	0.000
14	58101001	0.028	0.040	0.028	0.002	0.028	0.047	0.100	0.100	0.028	0.047
15	58101003	0.273	0.702	0.636	0.165	0.165	0.022	0.184	0.109	0.018	0.018
16	58101004	0.035	0.036	0.036	0.017	0.000	0.587	0.633	0.061	0.573	0.000
17	58101005	0.157	0.229	0.214	0.062	0.035	0.097	0.135	0.103	0.086	0.005
18	58201001	0.080	0.162	0.115	0.040	0.040	0.029	0.046	0.029	0.029	0.029
19	58501001	0.000	0.015	0.015	0.011	0.018	0.000	0.000	0.000	0.000	0.000
20	58701001	0.198	0.246	0.246	0.067	0.000	0.047	0.055	0.055	0.006	0.000
21	58701003	0.044	0.051	0.051	0.012	0.000	0.019	0.019	0.019	0.007	0.000
22	59001001	0.016	0.064	0.024	0.012	0.012	0.030	0.036	0.036	0.024	0.024
23	59301001	0.015	0.015	0.015	0.004	0.016	0.014	0.014	0.014	0.010	0.029
24	59301003	0.051	0.055	0.053	0.019	0.053	0.046	0.046	0.033	0.000	0.046
25	59301004	0.043	0.070	0.070	0.039	0.043	0.005	0.064	0.064	0.005	0.005
26	59301005	0.057	0.118	0.089	0.057	0.057	0.178	0.337	0.213	0.178	0.178
27	59401001	0.010	0.010	0.010	0.010	0.006	0.032	0.032	0.032	0.032	0.024
28	59401002	0.103	0.145	0.145	0.029	0.000	0.340	0.343	0.098	0.000	0.000
29	61101001	0.311	0.284	0.273	0.273	0.297	0.570	0.570	0.398	0.564	0.564
30	61601001	0.629	0.594	0.531	0.430	0.686	0.853	0.853	0.353	0.424	0.965
31	61601002	0.330	0.292	0.249	0.198	0.394	0.041	0.039	0.039	0.037	0.041
32	61601003	0.122	0.104	0.040	0.003	0.189	0.053	0.053	0.000	0.000	0.053
33	61601004	0.161	0.141	0.131	0.087	0.187	0.392	0.392	0.279	0.268	0.409
34	61601007	0.000	0.000	0.000	0.000	0.000	0.002	0.000	0.000	0.000	0.002
35	62301001	0.004	0.004	0.000	0.000	0.004	0.006	0.006	0.003	0.000	0.006
36	63201001	0.265	0.201	0.159	0.106	0.417	0.660	0.371	0.359	0.317	0.705
37	63201002	0.067	0.062	0.062	0.062	0.067	0.009	0.009	0.009	0.009	0.009

(*continued on next page*)

Table A3 (*continued*)

38	63201003	0.012	0.012	0.012	0.012	0.015	0.077	0.077	0.077	0.062	0.077
39	76801001	0.027	0.027	0.023	0.003	0.043	0.125	0.125	0.125	0.004	0.234
40	76801005	0.010	0.010	0.004	0.003	0.010	0.051	0.051	0.051	0.048	0.051
41	76801007	0.000	0.009	0.009	0.006	0.009	0.000	0.000	0.000	0.000	0.000
42	76801009	0.018	0.018	0.016	0.008	0.018	0.122	0.122	0.122	0.000	0.122
43	78501001	0.008	0.008	0.008	0.008	0.004	0.014	0.014	0.014	0.006	0.000
44	78501005	0.013	0.026	0.001	0.000	0.000	0.016	0.016	0.000	0.000	0.000
45	78601001	0.000	0.005	0.005	0.005	0.005	0.000	0.000	0.000	0.000	0.000
46	86101002	0.129	0.086	0.086	0.086	0.087	0.415	0.403	0.409	0.409	0.403
47	86101003	0.070	0.000	0.026	0.070	0.000	0.051	0.000	0.029	0.051	0.000
48	86101004	0.158	0.158	0.158	0.158	0.158	0.058	0.058	0.058	0.058	0.058
49	86101006	0.112	0.040	0.112	0.112	0.040	0.029	0.000	0.029	0.029	0.000
50	86101007	0.011	0.011	0.011	0.011	0.011	0.091	0.091	0.091	0.091	0.091
51	86101009	0.087	0.087	0.077	0.061	0.104	0.094	0.055	0.029	0.026	0.097
52	86104011	0.679	0.472	0.415	0.415	0.660	0.927	0.927	0.851	0.851	0.966
53	86501001	0.021	0.014	0.014	0.014	0.014	0.035	0.035	0.035	0.035	0.035
54	86801001	0.007	0.007	0.007	0.007	0.007	0.000	0.000	0.000	0.000	0.000
55	87001002	0.016	0.016	0.016	0.016	0.016	0.007	0.007	0.007	0.007	0.007
56	87001003	0.000	0.001	0.001	0.001	0.001	0.000	0.000	0.000	0.000	0.000
57	87601001	0.044	0.044	0.044	0.044	0.044	0.045	0.045	0.045	0.045	0.045
58	88301001	0.000	0.002	0.002	0.002	0.002	0.000	0.000	0.000	0.000	0.000
59	88401001	0.001	0.000	0.000	0.000	0.000	0.022	0.000	0.000	0.000	0.022
60	88401002	0.010	0.004	0.004	0.005	0.004	0.064	0.057	0.057	0.086	0.057
61	92901001	0.068	0.068	0.037	0.007	0.075	0.052	0.052	0.052	0.007	0.060
62	92901002	0.000	0.000	0.000	0.000	0.000	0.075	0.075	0.075	0.055	0.075
63	92901004	0.001	0.001	0.001	0.001	0.001	0.126	0.126	0.126	0.126	0.126
64	93401001	0.003	0.003	0.002	0.002	0.003	0.120	0.120	0.120	0.120	0.120
65	93401002	0.002	0.002	0.002	0.002	0.002	0.099	0.099	0.099	0.073	0.099
66	93801001	0.000	0.000	0.000	0.000	0.000	0.023	0.023	0.023	0.000	0.023
67	93801002	0.006	0.006	0.006	0.000	0.006	0.004	0.004	0.004	0.000	0.004
68	93801004	0.017	0.017	0.017	0.009	0.017	0.388	0.388	0.388	0.375	0.388
69	93901001	0.000	0.000	0.000	0.000	0.000	0.017	0.000	0.000	0.000	0.017
70	93901004	0.000	0.000	0.000	0.000	0.019	0.010	0.000	0.000	0.000	0.030
71	94201013	0.000	0.000	0.000	0.000	0.000	0.000	0.000	0.000	0.000	0.003
72	94201014	0.000	0.087	0.066	0.000	0.101	0.000	0.000	0.000	0.000	0.007
73	94201015	0.696	0.696	0.667	0.060	0.813	0.475	0.475	0.475	0.044	0.535
74	94201016	0.173	0.173	0.109	0.000	0.438	0.750	0.750	0.446	0.000	0.751
75	94201017	0.146	0.146	0.112	0.000	0.202	0.784	0.784	0.047	0.000	0.797
76	94201018	0.313	0.313	0.211	0.000	0.430	0.375	0.375	0.153	0.000	0.484
77	94201019	0.479	0.475	0.407	0.041	0.655	0.461	0.461	0.455	0.026	0.741
78	94201020	0.000	0.000	0.000	0.000	0.000	0.437	0.000	0.000	0.000	0.445
79	94201021	1.000	1.000	0.919	0.000	1.000	1.000	1.000	0.899	0.000	1.000
80	94201022	0.190	0.190	0.102	0.000	0.238	0.464	0.464	0.464	0.000	0.571
81	94201023	0.416	0.409	0.366	0.007	0.596	0.948	0.948	0.283	0.042	0.968
82	94201024	0.837	0.837	0.566	0.000	1.000	0.608	0.608	0.452	0.000	0.608
83	94201026	0.011	0.011	0.011	0.000	0.036	0.460	0.460	0.460	0.000	0.603
84	94201027	0.079	0.079	0.045	0.001	0.114	0.098	0.098	0.098	0.033	0.121
	Total no. of TZ affected	**66**	**74**	**72**	**61**	**68**	**74**	**65**	**65**	**51**	**69**

Table A4
Correlation coefficients before flood condition

	POP and A1	POP and A2	OPP and A1	OPP and A2
Spearman	**0.77 (p = 0)**	0.24 (p = 0)	0.31 (p = 0)	0.9 (p = 0)
Pearson	0.74 (p = 0)	−0.01 (p = 0.88)	0.26 (p = 0)	**0.97 (p = 0)**

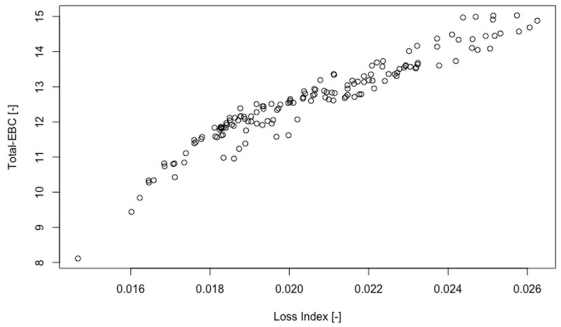

Fig. A1. Correlation of Loss Index and Total-EBC per 150 flood scenarios.

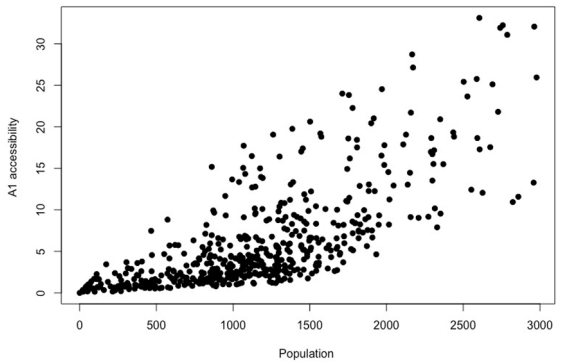

Fig. A2. Monotonous relationship between total population and A1 accessibility before the onset of floods. Monotonous relationship means when population increases, A1 accessibility increases in general. X-axis: population per traffic zone, Y-axis: A1 accessibility.

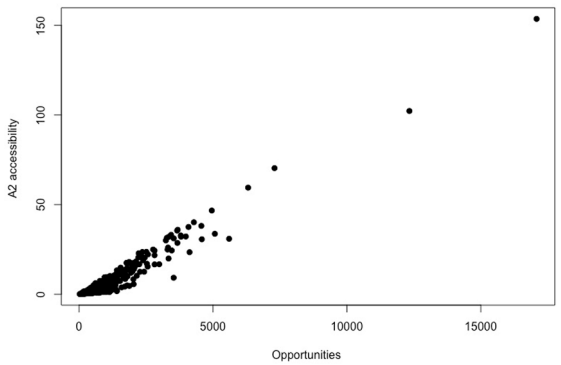

Fig. A3. Linear relationship between total opportunities and A2 accessibility before the onset of floods. X-axis: opportunities per traffic zone, Y-axis: A2 accessibility of a traffic zone.

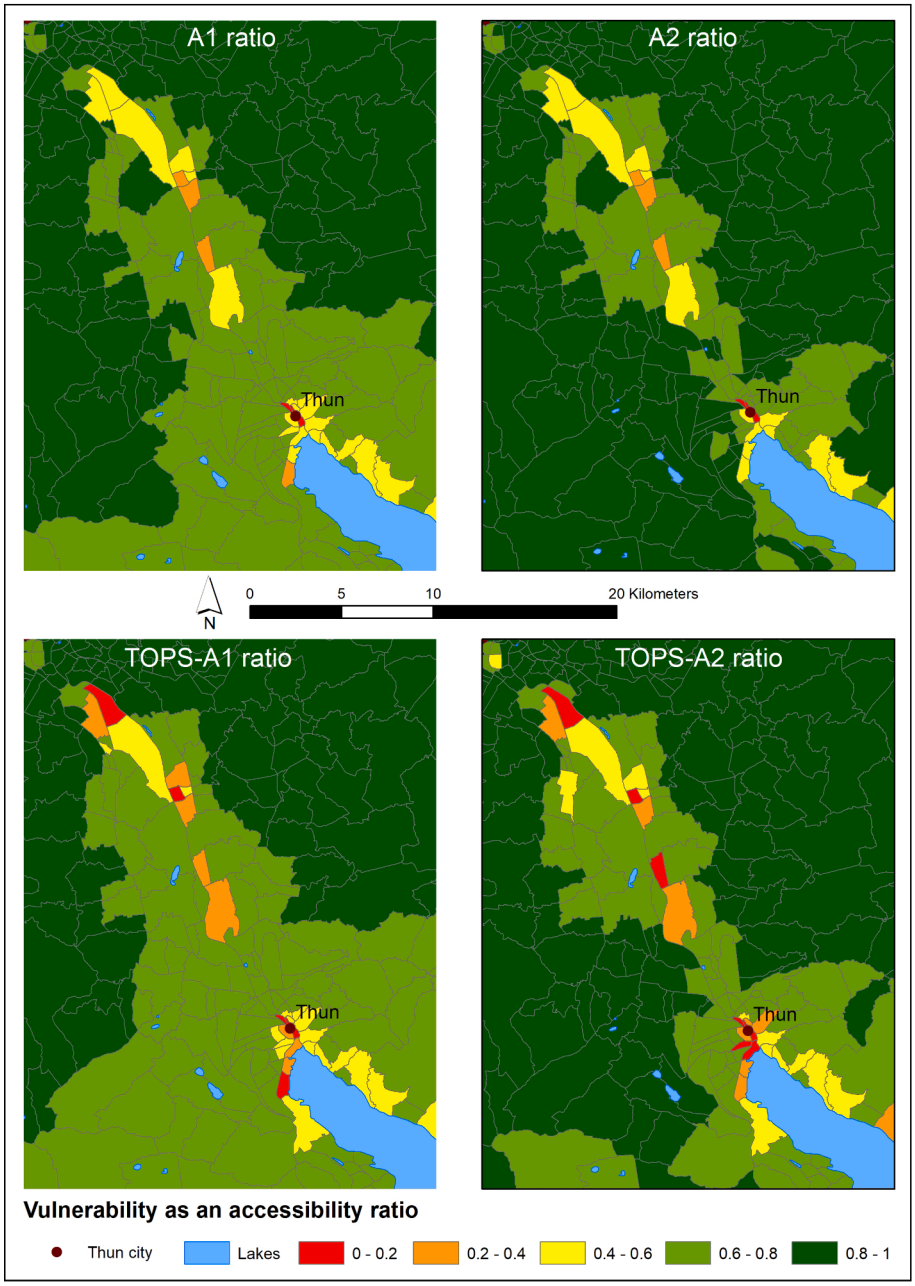

Fig. A4. Comparison among accessibility ratios of A1, TOPS-A1, A2, TOPS-A2 for f69 flood scenario. Different colours indicate the most vulnerable (red), and the least vulnerable (dark green) TZs. Map locations are indicated by red extent in Fig. 10.

References

Alfieri, L., Bisselink, B., Dottori, F., Naumann, G., de Roo, A.d., Salamon, P., Wyser, K., Feyen, L., 2017. Global projections of river flood risk in a warmer world. Earth's Futur. 5 (2), 171–182. https://doi.org/10.1002/2016EF000485.

ARE, 2020. Modelletablierung Nationales Personenverkehrsmodell (NPVM) 2017.

Basso, F., Frez, J., Martínez, L., Pezoa, R., Varas, M., 2020. Accessibility to opportunities based on public transport gps-monitored data: the case of Santiago. Chile. Travel Behav. Soc. 21, 140–153. https://doi.org/10.1016/j.tbs.2020.06.004.

Berdica, K., 2002. An introduction to road vulnerability: what has been done, is done and should be done. Transp. Policy 9 (2), 117–127. https://doi.org/10.1016/S0967-070X(02)00011-2.

Birkmann, J., Cardona, O.D., Carreno, M.L., Barbat, A.H., Pelling, M., Schneiderbauer, S., Kienberger, S., Keiler, M., Alexander, D., Zeil, P., Welle, T., 2013. Framing vulnerability, ris and societal responses: the MOVE framework. Nat. Hazards. https://doi.org/10.1007/s11069-013-0558-5.

Borowska-Stefańska, M., Kowalski, M., Wiśniewski, S., 2019. The measurement of mobility-based accessibility-the impact of floods on trips of various length and motivation. ISPRS Int. J. Geo-Inform. 8 (12), 534. https://doi.org/10.3390/ijgi8120534.

Bubeck, P., De Moel, H., Bouwer, L.M.H., Aerts, J.C.J., 2011. How reliable are projections of future flood damage? Nat. Hazards Earth Syst. Sci. 11, 3293–3306. https://doi.org/10.5194/nhess-11-3293-2011.
Bubeck, Philip, Dillenardt, Lisa, Alfieri, Lorenzo, Feyen, Luc, Thieken, Annegret H., Kellermann, Patric, 2019. Global warming to increase flood risk on European railways. Clim. Change 155 (1), 19–36. https://doi.org/10.1007/s10584-019-02434-5.
Cantillo, Victor, Macea, Luis F., Jaller, Miguel, 2019. Assessing vulnerability of transportation networks for disaster response operations. Networks Spat. Econ. 19 (1), 243–273. https://doi.org/10.1007/s11067-017-9382-x.
Casali, Y., Heinimann, H.R., 2019. A topological characterization of flooding impacts on the Zurich road network. PLoS One 14. https://doi.org/10.1371/journal.pone.0220338.
Casali, Y., Heinimann, H.R., 2019. A topological analysis of growth in the Zurich road network. Comput. Environ. Urban Syst. 75, 244–253. https://doi.org/10.1016/j.compenvurbsys.2019.01.010.
Caschili, Simone, Reggiani, Aura, Medda, Francesca, 2015. Resilience and vulnerability of spatial economic networks. Netw. Spat. Econ. 15 (2), 205–210. https://doi.org/10.1007/s11067-015-9283-9.
Chen, Xian-Zhe, Lu, Qing-Chang, Peng, Zhong-Ren, Ash, John Eugene, 2015. Analysis of transportation network vulnerability under flooding disasters. Transp. Res. Rec. J. Transp. Res. Board 2532 (1), 37–44. https://doi.org/10.3141/2532-05.
CRED and UNISDR, 2018. Economic Losses, Poverty and Disasters 1998–2017. https://doi.org/10.13140/RG.2.2.35610.08643.
Federal Office of Topography, 2019. swissTLM3D, https://shop.swisstopo.admin.ch/en/products/landscape/tlm3D.
Federal Statistical Office, 2017. Schools by educational level, https://www.bfs.admin.ch/bfs/en/home/statistics/education-science/educational-institutions/schools-educational-level.html.
Federal Statistical Office, 2016a. STATPOP, https://www.bfs.admin.ch/bfs/en/home/statistics/population/surveys/statpop.html.
Federal Statistical Office, 2016b. Structural business statistics. https://www.bfs.admin.ch/bfs/en/home/services/geostat/swiss-federal-statistics-geodata/business-employment/structural-business-statistics-statent-from-2011-onwards.assetdetail.5986776.html.
Fuchs, S., Keiler, M., Ortlepp, R., Schinke, R., Papathoma-Köhle, M., 2019. Recent advances in vulnerability assessment for the built environment exposed to torrential hazards: challenges and the way forward. J. Hydrol. 575, 587–595. https://doi.org/10.1016/j.jhydrol.2019.05.067.
Fuchs, S., Keiler, M., Zischg, A., 2015. A spatiotemporal multi-hazard exposure assessment based on property data. Nat. Hazards Earth Syst. Sci. 15, 2121–2142. https://doi.org/10.5194/nhess-15-2127-2015.
Fuchs, Sven, Röthlisberger, Veronika, Thaler, Thomas, Zischg, Andreas, Keiler, Margreth, 2017. Natural hazard management from a coevolutionary perspective: exposure and policy response in the European Alps. Ann. Am. Assoc. Geogr. 107 (2), 382–392. https://doi.org/10.1080/24694452.2016.1235494.
Geurs, Karst T., van Wee, Bert, 2004. Accessibility evaluation of land-use and transport strategies: review and research directions. J. Transp. Geogr. 12 (2), 127–140. https://doi.org/10.1016/j.jtrangeo.2003.10.005.
Girvan, M., Newman, M.E.J., 2002. Community structure in social and biological networks. Proc. Natl. Acad. Sci. U. S. A. 99, 7821–7826. https://doi.org/10.1073/pnas.122653799.
Gori, A., Gidaris, I., Elliott, J.R., Padgett, J., Loughran, K., Bedient, P., Panakkal, P., Juan, A., 2020. Accessibility and recovery assessment of Houston's roadway network due to fluvial flooding during hurricane Harvey. Nat. Hazards Rev. 21, 1–20. https://doi.org/10.1061/(ASCE)NH.1527-6996.0000355.
Grubesic, T.H., Matisziw, T.C., 2013. A typological framework for categorizing infrastructure vulnerability. Geo J. 78, 287–301. https://doi.org/10.1007/s10708-011-9411-0.
Hallegatte, S., Rentschler, J., Rozenberg, J., 2019. Lifelines. World Bank Group.
Hansen, Walter G., 1959. How accessibility shapes land use. J. Am. Plan. Assoc. 25 (2), 73–76. https://doi.org/10.1080/01944365908978307.
Hasan, S., Foliente, G., 2015. Modeling infrastructure system interdependencies and socioeconomic impacts of failure in extreme events: emerging R&D challenges. Nat. Hazards 78, 2143–2168. https://doi.org/10.1007/s11069-015-1814-7.
Hoegh-Guldberg, O., Jacob, D., Taylor, M., Bindi, M., Brown, S., Camilloni, I., Diedhiou, A., Djalante, R., Ebi, K.L., Engelbrecht, F., Guiot, J., Hijioka, Y., Mehrotra, S., Payne, A., Seneviratne, S.I., Thomas, A., Warren, R., 2018. Impacts of 1.5°C global warming on natural and human systems. In: Global Warming of 1.5°C. An IPCC Special Report on the Impacts of Global Warming of 1.5°C above Pre-Industrial Levels and Related Global Greenhouse Gas Emission Pathways, in the Context of Strengthening the Global Response to the Threat of Climate Change, pp. 175–311.
Jenelius, E., Mattsson, L.-G., 2015. Road network vulnerability analysis: conceptualization, implementation and application. Comput. Environ. Urban Syst. 49, 136–147. https://doi.org/10.1016/j.compenvurbsys.2014.02.003.
Jenelius, E., Peterson, T., Mattsson, L.-G., 2006. Importance and exposure in road network vulnerability analysis. Transp. Res. Part A 40, 537–560. https://doi.org/10.1016/j.tra.2005.11.003.
Kermanshah, A., Derrible, S., 2017. Robustness of road systems to extreme flooding: using elements of GIS, travel demand, and network science. Nat. Hazards 86, 151–164. https://doi.org/10.1007/s11069-016-2678-1.
Kermanshah, A., Derrible, S., Berkelhammer, M., 2017. Using climate models to estimate urban vulnerability to flash floods. J. Appl. Meteorol. Climatol. 56, 2637–2650. https://doi.org/10.1175/JAMC-D-17-0083.1.
Litman, T.A., 2008. Evaluating Accessibility for Transport Planning.
Malgwi, M.B., Fuchs, S., Keiler, M., 2020. A generic physical vulnerability model for floods: review and concept for data-scarce regions. Nat. Hazards Earth Syst. Sci. 20, 2067–2090. https://doi.org/10.5194/nhess-20-2067-2020.
Miller, Eric J., 2018. Accessibility: measurement and application in transportation planning. Transp. Rev. 38 (5), 551–555. https://doi.org/10.1080/01441647.2018.1492778.
Neumann, James E., Price, Jason, Chinowsky, Paul, Wright, Leonard, Ludwig, Lindsay, Streeter, Richard, Jones, Russell, Smith, Joel B., Perkins, William, Jantarasami, Lesley, Martinich, Jeremy, 2015. Climate change risks to US infrastructure: impacts on roads, bridges, coastal development, and urban drainage. Clim. Change 131 (1), 97–109. https://doi.org/10.1007/s10584-013-1037-4.
Noland, R.B., Wang, S., Kulp, S., Strauss, B.H., 2019. Employment accessibility and rising seas. Transp. Res. Part D Transp. Environ. 77, 560–572. https://doi.org/10.1016/j.trd.2019.09.017.
Papathoma-Köhle, M., Cristofari, G., Wenk, M., Fuchs, S., 2019. The importance of indicator weights for vulnerability indices and implications for decision making in disaster management. Int. J. Disaster Risk Reduct. 36, 101103. https://doi.org/10.1016/j.ijdrr.2019.101103.
Papilloud, Tsolmongerel, Röthlisberger, Veronika, Loreti, Simone, Keiler, Margreth, 2020. Flood exposure analysis of road infrastructure – comparison of different methods at national level. Int. J. Disaster Risk Reduct. 47, 101548. https://doi.org/10.1016/j.ijdrr.2020.101548.
Pearson, M., Hamilton, K., 2014. Investigating driver willingness to drive through flooded waterways. Accid. Anal. Prev. 72, 382–390. https://doi.org/10.1016/j.aap.2014.07.018.
Pregnolato, M., Ford, A., Wilkinson, S.M., Dawson, R.J., 2017. The impact of flooding on road transport: a depth-disruption function. Transp. Res. Part D 55, 67–81. https://doi.org/10.1016/j.trd.2017.06.020.
Pyatkova, K., Chen, A.S., Djordjević, S., Butler, D., Vojinović, Z., Abebe, Y.A., Hammond, M., 2015. Flood Impacts on Road Transportation Using Microscopic Traffic Modelling Techniques. https://doi.org/10.1007/978-3-319-33616-9_8.
Reggiani, A., Nijkamp, P., Lanzi, D., 2015. Transport resilience and vulnerability: the role of connectivity. Transp. Res. Part A Policy Pract. 81, 4–15. https://doi.org/10.1016/j.tra.2014.12.012.
Schlögl, Matthias, Richter, Gerald, Avian, Michael, Thaler, Thomas, Heiss, Gerhard, Lenz, Gernot, Fuchs, Sven, 2019. On the nexus between landslide susceptibility and transport infrastructure – an agent-based approach. Nat. Hazards Earth Syst. Sci. 19 (1), 201–219. https://doi.org/10.5194/nhess-19-201-201910.5194/nhess-19-201-2019-supplement.
Shi, Yuji, Blainey, Simon, Sun, Chao, Jing, Peng, 2020. A literature review on accessibility using bibliometric analysis techniques. J. Transp. Geogr. 87, 102810. https://doi.org/10.1016/j.jtrangeo.2020.102810.
Silva, C., Bertolini, L., Pinto, N. (Eds.), 2019. Designing Accessibility Instruments. Taylor & Francis Group.

Sohn, Jungyul, 2006. Evaluating the significance of highway network links under the flood damage: an accessibility approach. Transp. Res. Part A Policy Pract. 40 (6), 491–506. https://doi.org/10.1016/j.tra.2005.08.006.
Taylor, M.A.P., 2017. Vulnerability Analysis for Transportation Networks. Elsevier.
Taylor, M.A.P., 2008. Critical transport infrastructure in urban areas: Impacts of traffic incidents assessed using accessibility-based network vulnerability analysis. Growth Change. https://doi.org/10.1111/j.1468-2257.2008.00448.x.
Taylor, M.A.P., D'Este, G.M., 2007. Transport network vulnerability: a method for diagnosis of critical locations in transport infrastructure systems. In: Murray, A.T., Grubesic, T.H. (Eds.), Critical Infrastructure: Reliability and Vulnerability. Springer, Berlin, Heidelberg, pp. 9–30. https://doi.org/10.1007/978-3-540-68056-7.
Taylor, M.A.P., Sekhar, S.V.C., D'Este, G.M., 2006. Application of accessibility based methods for vulnerability analysis of strategic road networks. Netw. Spat. Econ. 6, 267–291. https://doi.org/10.1007/s11067-006-9284-9.
Taylor, M.A.P., Susiliwati, 2012. Remoteness and accessibility in the vulnerability analysis of regional road networks. Transp. Res. Part A 46, 761–771. https://doi.org/10.1016/j.tra.2012.02.008.
Thieken, A.H., Bessel, T., Kienzler, S., Kreibich, H., Müller, M., Pisi, S., Schröter, K., 2016. The flood of June 2013 in Germany: how much do we know about its impacts? Nat. Hazards Earth Syst. Sci. 16, 1519–1540. https://doi.org/10.5194/nhess-16-1519-2016.
UNISDR, 2016. Report of the open-ended intergovernmental expert working group on indicators and terminology relating to disaster risk reduction.
Unterrader, S., Almond, P., Fuchs, S., 2018. Rockfall in the Port Hills of Christchurch: seismic and non-seismic fatality risk on roads. N. Z. Geog. 74, 3–14. https://onlinelibrary.wiley.com/doi/10.1111/nzg.12170.
Wachs, Martin, Kumagai, T. Gordon, 1973. Physical accessibility as a social indicator. Socioecon. Plann. Sci. 7 (5), 437–456. https://doi.org/10.1016/0038-0121(73)90041-4.
Weaver, K.F., Morales, V.C., Dunn, S.L., Godde, K., Weaver, P.F., 2017. Pearson' s and Spearman's Correlation, in: An Introduction to Statistical Analysis in Research: With Applications in the Biological and Life Sciences. John Wiley & Sons, Inc. https://doi.org/10.1002/9781119454205.
Yin, J., Yu, D., Yin, Z., Liu, M., He, Q., 2016. Evaluating the impact and risk of pluvial flash flood on intra-urban road network: a case study in the city center of Shanghai. China. J. Hydrol. 537, 138–145. https://doi.org/10.1016/j.jhydrol.2016.03.037.
Zio, Enrico, 2016. Challenges in the vulnerability and risk analysis of critical infrastructures. Reliab. Eng. Syst. Saf. 152, 137–150.
Zischg, A., Fuchs, S., Keiler, M., Meißl, G., 2005a. Modelling the system behaviour of wet snow avalanches using an expert system approach for risk management on high alpine traffic roads. Nat. Hazards Earth Syst. Sci. 5, 821–832. https://doi.org/10.5194/nhess-5-821-2005.
Zischg, A., Fuchs, S., Keiler, M., Stötter, J., 2005b. Temporal variability of damage potential on roads as a conceptual contribution towards a short-term avalanche risk simulation. Nat. Hazards Earth Syst. Sci. 5, 235–242. https://doi.org/10.5194/nhess-5-235-2005.
Zischg, A.P., Felder, G., Weingartner, R., Quinn, N., Coxon, G., Neal, J., Freer, J., Bates, P., 2018. Effects of variability in probable maximum precipitation patterns on flood losses. Hydrol. Earth Syst. Sci. 22, 2759–2773. https://doi.org/10.5194/hess-22-2759-2018.